with second primary carcinoma were excluded from this series, because the endometrioid type and the others are referred to as type 1 and type 2 endometrial cancer are considered to originate from different mechanisms and exhibit different clinical behaviors.[17]

We also examined 12 sections of normal cyclic endometria derived from surgically resected specimens for benign uterine diseases, six of which were in the proliferative phase and six of which were in the secretory phase. The average age of these patients was 38.7 ± 4.9 and 40.3 ± 6.1 years, respectively. All specimens were routinely processed (i.e. 10% formalin fixed for 24–48 h), paraffin embedded, and thin sectioned (3 μm).

**Immunohistochemical staining and scoring of immunoreactivity.** We performed immunohistochemical staining for vasohibin, VEGFR-2, CD34 as a marker for vascular endothelial cells, and D2-40 as a lymphatic vessel marker. Ki-67 and VEGF-A were investigated in endometrial carcinoma cells. Paraffin-embedded tissue sections from human endometrial cancers were deparaffinized, rehydrated, and incubated with 3% $H_2O_2$ for 10 min to block endogenous peroxidase activity. Sections were incubated for 30 min at room temperature (RT) in a blocking solution of 10% goat serum (Nichirei Biosciences, Tokyo, Japan), and then stained for 12 h at 4°C with primary antibodies, followed by staining for 30 min at RT with secondary antibodies. The primary antibodies were all mouse monoclonal antibodies and were used as follows: 2 μg/mL antihuman vasohibin monoclonal antibody, anti-VEGFR-2 (Santa Cruz Biotechnology, Santa Cruz, CA, USA) diluted 1:100, anti-CD34 (Dako, Copenhagen, Denmark) diluted at 1:200, Ki-67 (Dako) diluted 1:100, anti-D2-40 (Dako) diluted 1:100, and anti-VEGF-A (Lab Vision, Fremont, CA, USA) diluted 1:100. We have previously described a mouse monoclonal antibody against a synthetic peptide corresponding to the 286–299 amino acid sequence of vasohibin.[13] The positive control slide for CD34 antigen was prepared from paraffin-fixed breast cancer tissue that was known to contain a high microvessel density. Nuclei were counterstained with hematoxylin.

Three investigators (A.T., H.T., M.K.) independently evaluated the immunohistochemical staining of the tissue sections. They were blinded to the clinical course of the patients and the average of the numbers counted by the three investigators was adopted for subsequent analysis. We carefully selected for investigation areas where cancer cells came into contact with or invaded into the stroma. First, microvessels were counted by searching for CD34-positive signals after scanning the immunostained section at low magnification. The areas with the greatest number of distinctly highlighted microvessels were selected. Any cell clusters with CD34-positive signals were regarded as a single countable microvessel, regardless of whether a lumen was visible or not. Unstained lumina were considered artifacts even if they contained blood or tumor cells. Microvessel density (MVD) was assessed by light microscopy in areas of invasive tumor containing the highest numbers of capillaries and small venules per area (neovascular hot spots) according to the original method.[19] In endometrioid adenocarcinoma, the ratio of stroma per total area (as neovascular hot spots) decreased significantly with poorer histological differentiation. Thus, we measured the ratio of stroma per total area using National Institute of Health imaging (200 × magnification hot spot picture captured with Nikon imaging) and revised the true vessel counts per 1 $mm^2$ of stroma (microvessel density) for each case.

Investigation of lymphatic vessel density (LVD) was performed using the same procedure described as above, by searching for D2-40-positive signals.

Next, immunostaining for vasohibin and VEGFR-2 was evaluated in serial thin sections. Positive immunoreactive signals for vasohibin and VEGFR-2 in the CD34-positive microvessels were counted and calculated as positive ratios of vasohibin and VEGFR-2 in microvessels. Evaluation of Ki-67 immunoreactivity was performed at high-power field (400X) and used as a marker of cell proliferation. More than 500 tumor cells from each of three different representative fields were counted and the percentage of the number of positively stained nuclei relative to the total numbers of cells were determined as a labeling index (LI). The protein expression of selected angiogenic factor (VEGF-A) was examined by immunohistochemistry using an established antibody. For this marker, cytoplasmic staining intensity and the proportion of positive tumor cells were recorded and a staining index (values of 0–9) was calculated as the product of staining intensity (0–3) and the area of positive staining (1, <10%; 2, 10–50%; 3, > 50%).[20]

**Statistical analysis.** Statistical analysis, such as the Student's *t*-test and Peason's correlation coefficient test, were performed using StatView (version 4.5; SAS Institute Inc., Cary, NC, US). The results were considered significant when the *P*-values were <0.05.

## Results

**Microvessel density of endometrioid adenocarcinoma.** CD34-positive microvessel density (counts per $mm^2$) were 41.1 ± 3.1, 36.9 ± 2.3, and 29.7 ± 1.7 in G1, G2, and G3, respectively; 35 ± 2.70 in the proliferative phase; and 36.3 ± 1.83 in the secretory phase (Figs 1 and 2). We measured the ratio of the stromal area per total hot spot area in the location with the greatest number of distinctly highlighted microvessels. In G1, the ratio was 32.7% ± 0.24; in G2, 27.5% ± 0.19; in G3, 5.8% ± 0.05; 73.2% ± 2.70 in the proliferative phase; and 70.0% ± 1.83 in the secretory phase. The ratio of the stromal area per total area of G3 was significantly lower than that of G1 and G2. CD34-positive microvessel density (counts per $mm^2$), as revised by the ratio of the stroma per total area, was 141.65 ± 13.2 in G1, 168.62 ± 19.38 in G2, and 788.94 ± 105.8 in G3, respectively; 48.71 ± 2.70 in the proliferative phase; and 52.45 ± 1.83 in the secretory phase. The MVD of G3 was significantly higher than the MVD of G1 and G2 (Fig. 3a).

**Lymphatic vessel density of endometrioid adenocarcinoma.** D2-40 positive lymphatic vessel density (counts per $mm^2$) was 4.73 ± 0.70 in G1, 8.83 ± 2.24 in G2, and 2.88 ± 0.54 in G3, respectively; 1.80 ± 0.20 in the proliferative phase; and 6.10 ± 0.50 in the secretory phase (Figs 1 and 2). D2-40 positive lymphatic vessel density (counts per $mm^2$), as revised by the ratio of stroma per total area, was 15.90 ± 2.30 in G1, 9.47 ± 1.95 in G2, and 91.01 ± 23.06 in G3, respectively; 2.53 ± 0.36 in the proliferative phase; and 8.83 ± 0.82 in the secretory phase. The LVD of G3 was significantly higher than the LVD of G1 and G2 (Fig. 3b).

**Vasohibin expression in microvessels in endometrial tissues.** The positive ratios of vasohibin in microvessels were 31.4% and 43.1% in the proliferative and secretory phases, respectively (Fig. 2). The positive ratios were significantly different between the two phases (Fig. 4a). In addition, the endothelium of the spiral arteries characteristically exhibited positivity in the secretory phase; the positive ratio of vasohibin was 95.4% and the positive ratio of VEGFR-2 was 87.4%. (Fig. 2).

The positive ratio of vasohibin in microvessels was 56.6% ± 12.8 in the endometrioid adenocarcinoma cases examined. Interestingly, the positive ratios differed according to grade: 52.5 ± 13.9 in G1 (well differentiated), 57.8% ± 13.5 in G2 (moderately differentiated), and 59.9% ± 10.0 in G3 (poorly differentiated) (Fig. 1). The positive ratio of vasohibin in microvessels in G3 was significantly higher than that in G1 (Fig. 4a). Positive ratios of vasohibin in microvessels in each histlogical grade were significantly higher than that of the proliferative phase ($P < 0.05$). Positive ratios were compared in clinical stages: 56.2% ± 11.2 in stage 1, 61.9% ± 15.5 in stage 2,

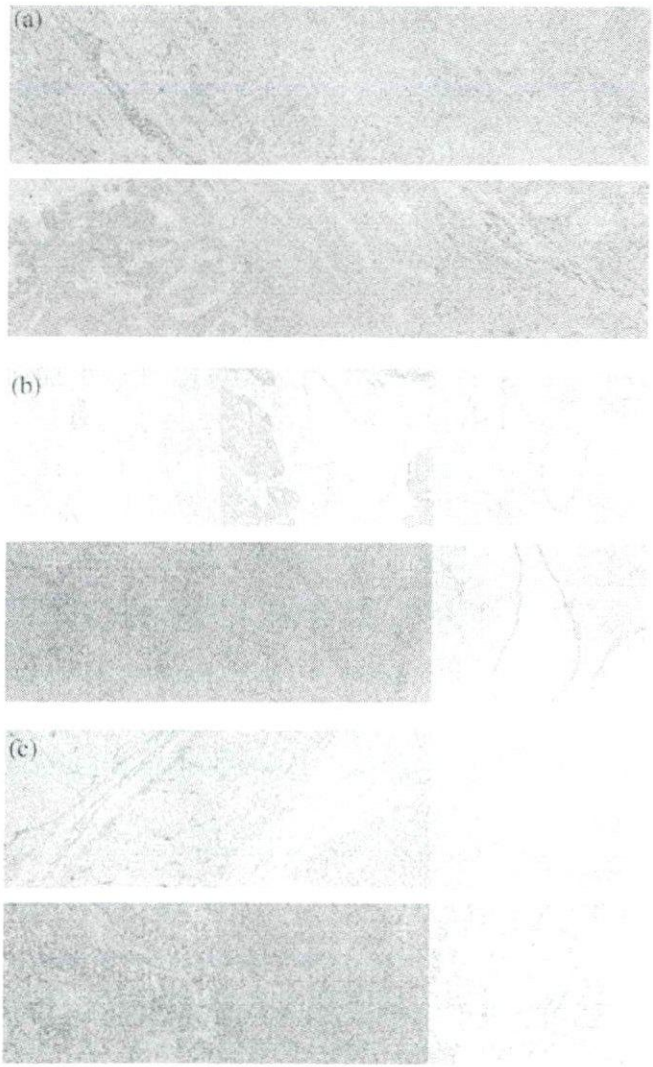

Fig. 1. (a) Immunohistochemistry in well-differentiated endometrioid adenocarcinomas. All sections stained positively for CD34 (upper left, original magnification 200×), vascular endothelial growth factor receptor-2 (VEGFR-2) (upper middle, original magnification 200×), vasohibin (upper right, original magnification 200× and lower right, original magnification 400×), and vascular endothelial growth factor-alpha (VEGF-A) (lower left, original magnification 200×). D2-40 (lower middle, original magnification 200×). (b) Immunohistochemistry in moderately differentiated adenocarcinoma. All sections stained positively as for (a). (c) Immunohistochemistry in poorly differentiated adenocarcinoma. All sections stained positively as for (a).

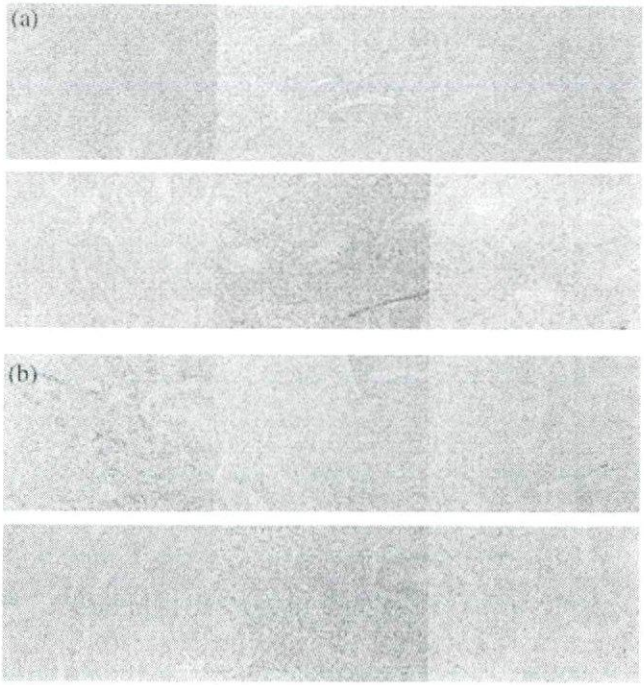

Fig. 2. (a) Immunohistochemistry in proliferative phase of cyclic endometria. All sections stained positively for CD34 (upper left, original magnification 200×), vascular endothelial growth factor receptor-2 (VEGFR-2) (upper middle, original magnification 200×), vasohibin (upper right, original magnification 200× and lower right, original magnification 400×), and vascular endothelial growth factor-alpha (VEGF-A) (lower left, original magnification 200×). D2-40 (lower middle, original magnification 200×). (b) Immunohistochemistry in secretory phase of cyclic endometria. All sections stained positively as for (a). Immunopositivity was significantly different between the two phases for vasohibin and VEGFR-2. The endothelium of the spiral arteries exhibited characteristic positivities in the secretory phase.

56.7% ± 12.9 in stage 3, and 57.7% ± 21.3 in stage 4. There was no significant difference between each group.

**VEGFR-2 expression in microvessels in endometrial tissues.** The VEGFR-2 positive ratio of the microvessels was 8.6% ± 1.0 and 22.5% ± 3.0 in the proliferative and secretory phases, respectively (Fig. 2). VEGFR-2 positive vessel ratio in the proliferative phase was significantly higher than in the secretory phase (Fig. 4b).

VEGFR-2 positive ratios in G1, 2, and G3 were 22.3% ± 13.0, 39.8% ± 12.8, and 47.6% ± 11.5, respectively (Fig. 1). The VEGFR-2 positive ratio in G2 was significantly higher than in G1 and cyclic endometria. The VEGFR-2 positive ratio in G3 was significantly higher than those of G1 and G2 (Fig. 4b). Positive ratios were compared between clinical stages: 32.8% ± 15.4% in stage 1, 33.9% ± 19.0 in stage 2, 37.5% ± 15.1 in stage 3, and 46.4% ± 16.8 in stage 4. There was no significant difference between each group.

**VEGF-A expression in endometrial tissues.** VEGF-A expression was detected in the cytoplasm of epithelial cells. The staining index of VEGF-A is shown in Figure 5. The VEGF-A positive ratio of cytoplasmic staining intensity was 0.67 ± 0.49 and 2.33 ± 0.76 in the proliferative and secretory phases, respectively (Fig. 5). In endometrioid adenocarcinomas VEGF-A positive ratios of cytoplasmic staining in grades 1, 2, and 3 were 3.85 ± 0.39, 4.2 ± 0.37, and 5.88 ± 0.37, respectively (Fig. 5). The VEGF-A positive ratio in G3 was significantly higher than in G1 and 2. The VEGF-A positive ratio in the proliferative phase was significantly lower than G1, G2, and G3, respectively, and the VEGF-A positive ratio in secretory phase was significantly lower than G2 and G3, respectively.

**Correlation between vasohibin and VEGFR-2 positive ratios in microvessels, and cell proliferation and expression of angiogenic factor.** A strongly positive correlation was found between vasohibin and VEGFR-2 positive ratios in microvessels in endometrioid adenocarcinomas ($P < 0.0001$, $r^2 = 0.591$) (Fig. 6).

We then analyzed vasohibin and VEGFR-2 positive ratios in comparison to cell proliferation and expression of angiogenic factor. The ratios of both vasohibin- and VEGFR-2-positivity did not correlate significantly to the LI of Ki-67 (data not



doi: 10.1111/j.1349-7006.2008.00777.x

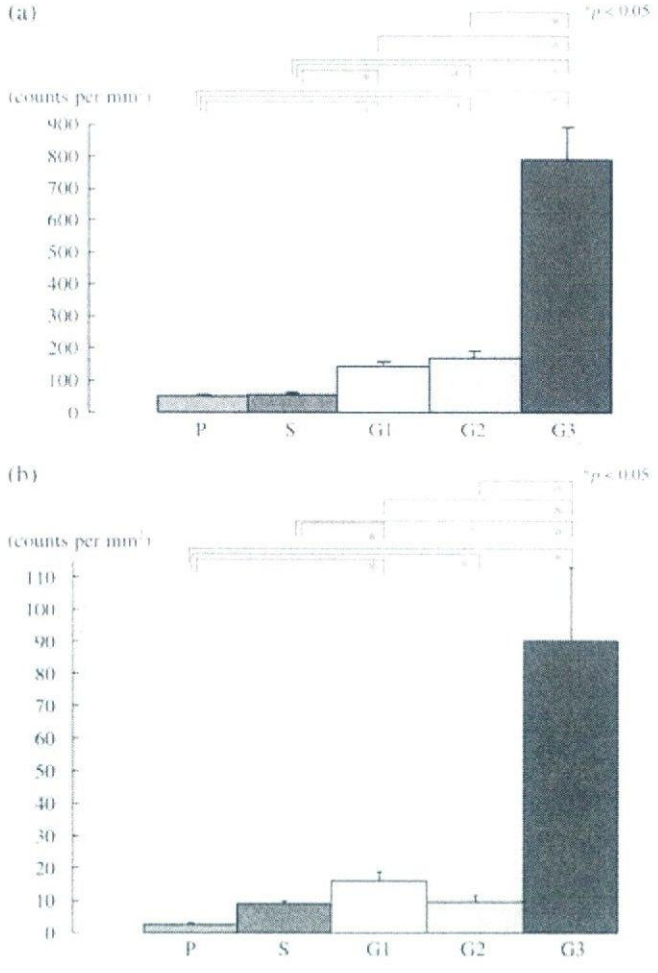


**Fig. 3.** (a) Microvessel density of cyclic endometria and endometrioid adenocarcinoma. Microvessel density of G3 was significantly higher than that of G1 and G2. G1, well-differentiated adenocarcinoma; G2, moderately differentiated adenocarcinoma; G3, poorly differentiated adenocarcinoma, $*P < 0.05$. (b) Lymphatic vessel density of cyclic endometria and endometrioid adenocarcinoma. Lymphatic vessel density of G3 was significantly higher than that of G1 and G2. G1, well-differentiated adenocarcinoma; G2, moderately differentiated adenocarcinoma; G3, poorly differentiated adenocarcinoma, $*P < 0.05$.

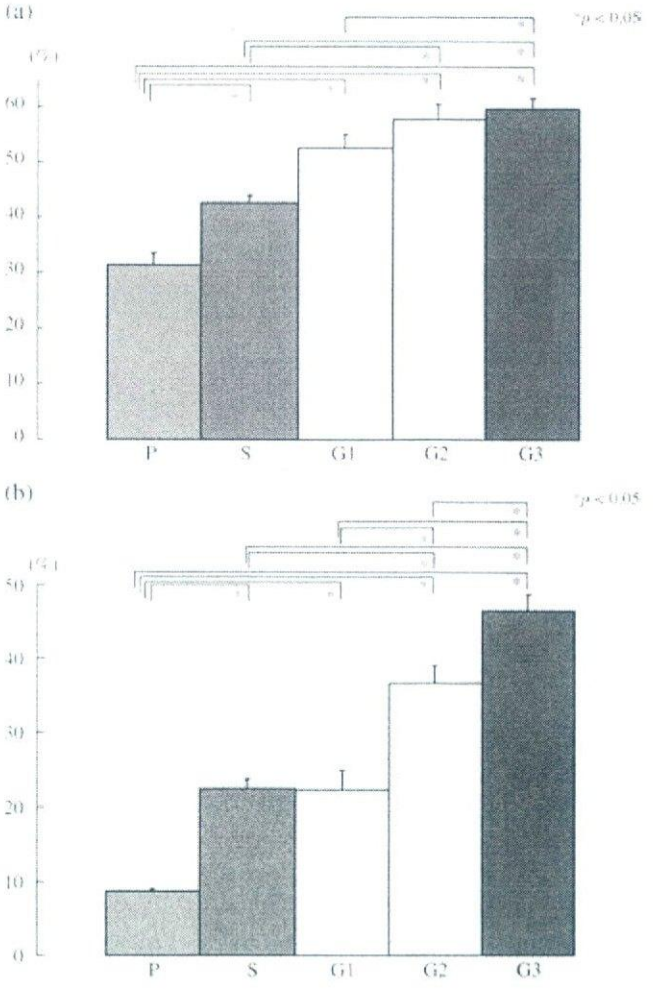


**Fig. 4.** (a) Proportion of vasohibin/CD34-positive vessels in cyclic endometria and endometrioid adenocarcinoma. Vasohibin-immunopositivity in microvessels in G3 was significantly higher than that in G1. S, secretory phase; P, proliferative phase; G1, well-differentiated adenocarcinoma; G2, moderately differentiated adenocarcinoma; G3, poorly differentiated adenocarcinoma, $*P < 0.05$. (b) Proportion of vascular endothelial growth factor receptor-2 (VEGFR-2)/CD34-positive vessels in cyclic endometria and endometrioid adenocarcinoma. VEGFR-2-immunopositivity of vessels in the proliferative phase was significantly higher than in the secretory phase. S, secretory phase; P, proliferative phase; G1, well-differentiated adenocarcinoma; G2, moderately differentiated adenocarcinoma; G3, poorly differentiated adenocarcinoma, $*P < 0.05$.

shown). No significant correlation was observed between the vasohibin- and VEGFR-2-positive ratios and VEGF-A expression in endometrioid adenocarcinoma (data not shown).

## Discussion

Here we examined the vascular density of endometrial cancer and compared it with that of normal endometrium. Some reports have previously indicated that MVD of endometrial cancer increases from well differentiated to poorly differentiated adenocarcinomas[4,21,22] but this relationship is not universally accepted.[23] Moreover, most of them have failed to consider the vessel numbers in normal endometrium and to compare it with those of adenocarcinoma. In the present study, we confirmed that the vessel number increased from normal endometrium to endometrial cancer, and that this increase was significantly augmented in poorly differentiated adenocarcinoma.

Recently, focus has been given to the importance of lymphangiogenesis for tumor metastasis.[24,25] Here, we investigated LVD in normal endometrium and endometrioid adenocarcinoamas. Our analysis revealed that LVD increased significantly in poorly differentiated adenocarcinoma, similar to MVD. Some studies have reported the presence of peritumoral lymphatic vessels in 40% of the cases in endometrial cancer and demonstrated that high LVD was strongly associated with the features of aggressive endometrial carcinomas, including high histological grade, presence of necrosis, and vascular invasion by tumor cells.[26–28] Although it was expected that frequent LVD correlated with lymph node metastasis, there was no significant correlation between LVD and lymph node metastasis. In the present study, only two cases out of 78 cases exhibited lymph node metastasis. Therefore, investigation of a greater number of cases with lymph node metastasis in endometrioid adenocarcinoma will be necessary to further elucidate this correlation. The

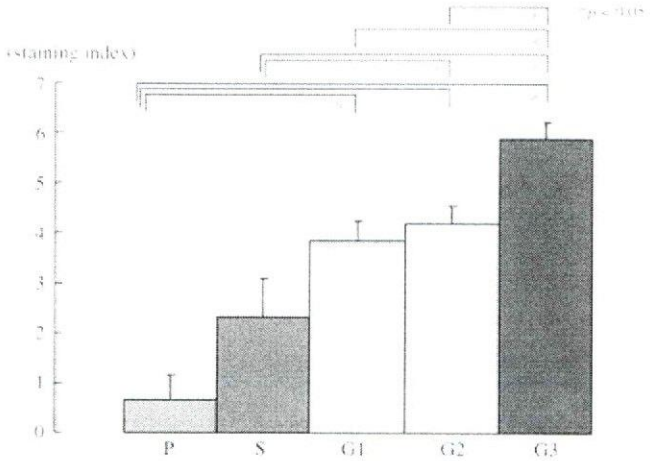


Fig. 5. Vascular endothelial growth factor-alpha (VEGF-A) staining indexes of the cytoplasm of the tumor cell and cyclic endometrial glands. *$P < 0.05$.

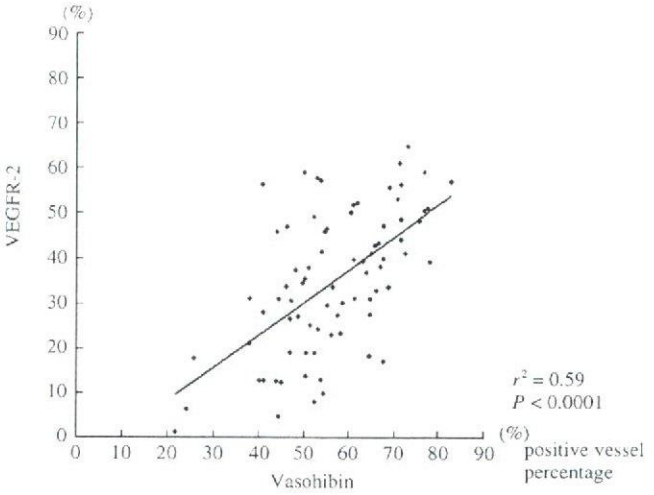


Fig. 6. Correlation between vasohibin and vascular endothelial growth factor receptor-2 (VEGFR-2). A strongly positive correlation was found between vasohibin- and VEGFR2-positive ratios in microvessels in endometrioid adenocarcinomas ($P < 0.0001$, $r^2 = 0.591$).

mechanism of the alteration of lymphangiogenesis from cyclic endometria to endometrioid adenocarcinoma remains unclear. Our analysis of MVD and LVD demonstrated that the secretory phase is similar to well differentiated and moderately differentiated endometrioid adenocarcinomas, which suggests that the function of cyclic endometria may be retained until adenocarcinomas become moderately differentiated.

We then examined the expression of vasohibin. Vasohibin is an endogenous endothelium-derived angiogenesis inhibitor that we have previously isolated.[13] Here we confirmed that the expression of vasohibin was restricted to vascular endothelium, and further observed that the ratio of vasohibin-positive vessels increased from normal endometrium to poorly differentiated adenocarcinomas. This is the first study to profile the expression of vasohibin in human gynecologic malignancy.

Several clinicopathologic studies have demonstrated a direct association between VEGF expression and increased MVD in human solid tumors, including breast[29] lung,[30] and gastric[31] malignancies. A similar association has been reported for normal[32] and malignant endometrium.[33–35] Between the two VEGF signal transducing receptors, VEGFR-2 transduces most of the angiogenesis-related signals in ECs. The VEGF/VEGFR-2 signaling pathway is also important for the induction of vasohibin in ECs.[16] We previously revealed that the VEGF-A-mediated induction of vasohibin was preferentially mediated via the VEGFR-2 signaling pathway.[16]

Our present analysis revealed that the ratio of VEGFR-2-positive vessels, as well as the ratio of vasohibin-positive vessels, also increased from normal endometrium to poorly differentiated endometrial adenocarcinomas. In addition, a significantly positive correlation existed between the positive ratios of vasohibin and VEGFR-2 expression in endometrioid endometrial carcinomas. This is the first study to elucidate this correlation between expression of these factors in human cancer. This result suggested the value of vasohibin as a biomarker of angiogenesis at least in endometrial cancer.

Angiogenesis is determined by the local balance between angiogenic stimulators and inhibitors. Therefore, one may anticipate the application of angiogenesis inhibitors towards antiangiogenic therapy for the treatment of human malignancies including endometrial cancer. A number of angiogenesis inhibitors have been investigated and identified, including pigment epithelium-derived factor (PEDF), angiostatin, endostatin, and thrombospondin-1 (TSP-1). Vasohibin is a newly identified negative feedback regulator for angiogenesis. We previously reported that transfection of Lewis lung carcinoma (LCC) cells with the vasohibin gene did not affect the proliferation of cancer cell *in vitro*, but did inhibit tumor growth and tumor angiogenesis *in vivo*.[13] The growth of vasohibin-producing LLC cells in mice was significantly attenuated. In addition, tumors of mock-transfectants contained large luminal vessels, whereas those of vasohibin-producing LLC cells contained very small vessels, even when the size of tumors did not differ extremely.[14] These results suggest that vasohibin may play a very important role in regulating tumor angiogenesis.

Among the various angiogenesis inhibitors, thrombospondin-1 (TSP-1) has been extensively studied in cancers, although the role of TSP-1 in endometrial tumor angiogenesis and progression still remains controversial.[36] The expression of TSP-1 in epithelial cells and/or caner cells is up-regulated by the tumor suppressor gene *p53*, and down-regulated by oncogenes such as Myc and Ras. Thus, the mutation of *p53* or activation of *myc* and *ras* results in the down-regulation of TSP-1, which may alter tumor growth by modulating angiogenesis in a variety of tumor types. Herein, we demonstrated that the expression of vasohibin increased in ECs of endometrial cancer. As the expression of vasohibin was restricted to normal ECs, the alteration of tumor suppressor gene and/or oncogenes in tumor cells would not influence the expression of vasohibin. However, angiogenesis inhibitors may function in a concerted manner. Therefore, vasohibin alone may not be sufficient to control tumor angiogenesis, if other inhibitors become deregulated.

Nevertheless, since the expression of vasohibin increased in correlation with that of VEGFR-2, vasohibin could be an important biomarker of angiogenesis in both normal endometrium and endometrial cancer. However, further investigations are required to clarify the precise roles of vasohibin in regulating antiangiogenic activity in normal endometrium and its disorders.

## Acknowledgments

This study was supported by a grant-in-aid from the Kurokawa Cancer Research Foundation; a grant-in-aid for Scientific Research on Priority Areas from the Ministry of Education, Science, and Culture of Japan; a grant-in-aid from the Ministry of Health, Labor, and Welfare of Japan; and a 21st Century COE Program Special Research Grant (Tohoku University) from the Ministry of Education, Science, Sports, and Culture of Japan.



doi: 10.1111/j.1349-7006.2008.00777.x

## References


1 Jemal A, Tiwari RC, Murray T *et al.* Cancer statistics, 2004. *CA Cancer J Clin* 2004; **54**: 8–29.
2 Abulafia O, Triest WE, Sherer DM, Hansen CC, Ghezzi F. Angiogenesis in endometrial hyperplasia and stage I endometrial carcinoma. *Obstet Gynecol* 1995; **86** (4): 479–85.
3 Kirschner CV, Alanis-Amezcua JM, Martin VG *et al.* Angiogenesis factor in endometrial carcinoma. a new prognostic indicator? *Am J Obstet Gynecol* 1996; **174**: 1879–82; discussion 1882–4.
4 Kaku T, Kamura T, Kinukawa N *et al.* Angiogenesis in endometrial carcinoma. *Cancer* 1997; **80**: 741–7.
5 Salvesen HB, Iversen OE, Akslen LA. Independent prognostic importance of microvessel density in endometrial carcinoma. *Br J Cancer* 1998; **77**: 1140–4.
6 de Gois Speck NM, Focchi J, Alves AC, Ribalta JC, Osorio CA. Relationship between angiogenesis and grade of histologic differentiation in endometrial adenocarcinoma. *Eur J Gynaecol Oncol* 2005; **26**: 599–601.
7 Stefansson IM, Salvesen HB, Akslen LA. Vascular proliferation is important for clinical progress of endometrial cancer. *Cancer Res* 2006; **66**: 3303–9.
8 Hirai M, Nakagawara A, Oosaki T, Hayashi Y, Hirono M, Yoshihara T. Expression of vascular endothelial growth factors (VEGF-A/VEGF-1 and VEGF-C/VEGF-2) in postmenopausal uterine endometrial carcinoma. *Gynecol Oncol* 2001; **80**: 181–8.
9 Fujisawa T, Watanabe J, Akaboshi M, Ohno E, Kuramoto H. Immunohistochemical study on VEGF expression in endometrial carcinoma – comparison with p53 expression, angiogenesis, and tumor histologic grade. *J Cancer Res Clin Oncol* 2001; **127**: 668–74.
10 Holland CM, Day K, Evans A, Smith SK. Expression of the VEGF and angiopoietin genes in endometrial atypical hyperplasia and endometrial cancer. *Br J Cancer* 2003; **89**: 891–8.
11 Saito M, Watanabe J, Fujisawa T *et al.* Angiopoietin-1, 2 and Tie2 expression in endometrial adenocarcinoma – the Ang2 dominant balance up-regulates tumor angiogenesis in the presence of VEGF. *Eur J Gynaecol Oncol* 2006; **27**: 129–34.
12 Mazurek A, Kuc P, Terlikowski S, Laudanski T. Evaluation of tumor angiogenesis and thymidine phosphorylase tissue expression in patients with endometrial cancer. *Neoplasma* 2006; **53**: 242–6.
13 Watanabe K, Hasegawa Y, Yamashita H *et al.* Vasohibin as an endothelium-derived negative feedback regulator of angiogenesis,. *J Clin Invest* 2004; **114**: 898–907.
14 Sonoda H, Ohta H, Watanabe K, Yamashita H, Sato Y. Multiple processing forms and their biological activities of a novel angiogenesis inhibitor Vasohibin. *Biochem Biophys Res Comms* 2006; **342**: 640–6.
15 Shibuya M, Claesson-Welsh L. Signal transduction by VEGF receptors in regulation of angiogenesis and lymphangiogenesis. *Exp Cell Res* 2006; **312**: 549–60.
16 Shimizu K, Watanabe K, Yamashita H *et al.* Gene regulation of a novel angiogenesis inhibitor, Vasohibin, in endothelial cells. *Biochem Biophys Res Commun* 2005; **327**: 700–6.
17 World Health Organization classification of tumours. In: Tavassoli FA, Devilee P, eds. *Pathology and Genetics of Tumours of the Breast and Female Genital Organs*. Lyon: IARC Press, 2003; 217–32.
18 Creasman WT. Announcement FIGO stages: 1988 revisions. *Gynecol Oncol* 1989; **35**: 125–7.
19 Weidner N, Semple JP, Welch WR, Folkman J. Tumor angiogenesis and metastasis – correlation in invasive breast carcinoma. *N Engl J Med* 1991; **324**: 1–8.
20 Aas T, Borresen AL, Geisler S *et al.* Specific P53 mutations are associated with de novo resistance to doxorubicin in breast cancer patients. *Nat Med* 1996; **2**: 811–4.
21 Wagatsuma S, Konno R, Sato S, Yajima A. Tumor angiogenesis, hepatocyte growth factor, and c-Met expression in endometrial carcinoma. *Cancer* 1998; **82**: 520–30.
22 Salvesen HB, Iversen OE, Akslen LA. Prognostic significance of angiogenesis and Ki-67, 53, and p21 expression: a population-based endometrial carcinoma study. *J Clin Oncol* 1999; **17**: 1382–90.
23 Morgan KG, Wilkinson N, Buckley CH. Angiogenesis in normal, hyperplastic, and neoplastic endometrium. *J Pathol* 1996; **179**: 317–20.
24 Alitalo K, Mohla S, Ruoslahti E. Lymphangiogenesis and cancer: meeting report. *Cancer Res* 2004; **64**: 9225–9.
25 Sipos B, Klapper W, Kruse ML *et al.* Expression of lymphangiogenic factors and evidence of intratumoral lymphangiogenesis in pancreatic endocrine tumors. *Am J Pathol* 2004; **165**: 1187–97.
26 Ingunn M, Stefansson Helga Salvesen B &, Lars Akslenl A. Vascular proliferation is important for clinical progress of endometrial cancer. *Cancer Res* 2006; **66**: 3303–7.
27 Bono P, Wasenius VM, Heikkila P *et al.* High LYVE-1-positive lymphatic vessel numbers are associatedwith poor outcome in breast cancer. *Clin Cancer Res* 2004; **10**: 7144–9.
28 Shields JD, Borsetti M, Rigby H *et al.* Lymphatic density and metastatic spread in human malignant melanoma. *Br J Cancer* 2004; **90**: 693–700.
29 Toi M, Inada K, Suzuki H, Tominaga T. Tumor angiogenesis in breast cancer: its importance as a prognostic indicator and the association with vascular endothelial growth factor expression. *Breast Cancer Res Treat* 1995; **36**: 193–204.
30 Giatromanolaki A, Koukourakis MI, Kakolyris S *et al.* Vascular endothelial growth factor, wild-type p53, and angiogenesis in early operable nonsmall cell lung cancer. *Clin Cancer Res* 1998; **4**: 3017–24.
31 Giatromanolaki A, Koukourakis MI, Stathopoulos GP *et al.* Angiogenic interactions of vascular endothelial growth factor, of thymidine phosphorylase, and of p53 protein expression in locally advanced gastric cancer. *Oncol Res* 2000; **12**: 33–41.
32 Charnock-Jones DS, Sharkey AM, Rajput-Williams J *et al.* Identification and localization of alternately spliced mRNAs for vascular endothelial growth factor in human uterus and estrogen regulation in endometrial carcinoma cell lines. *Biol Reprod* 1993; **48**: 1120–8.
33 Guidi AJ, Abu-Jawdeh G, Tognazzi K, Dvorak HF, Brown LF. Expression of vascular permeability factor (vascular endothelial growth factor) and its receptors in endometrial carcinoma. *Cancer* 1996; **78**: 454–60.
34 Fine BA, Valente PT, Feinstein GI, Dey T. VEGF, flt-1, and KDR/flk-1 as prognostic indicators in endometrial carcinoma. *Gynecol Oncol* 2000; **76**: 33–9.
35 Fujimoto J, Ichigo S, Hirose R, Sakaguchi H, Tamaya T. Expressions of vascular endothelial growth factor (VEGF) and its mRNA in uterine endometrial cancers. *Cancer Lett* 1998; **134**: 15–22.
36 Ren B, Yee KO, Lawler J, Khosravi-Far R. Regulation of tumor angiogenesis by thrombospondin-1. *Biochim Biophys Acta* 2006; **1765**: 178–88.

The EMBO Journal (2008) 27, 522–534 | © 2008 European Molecular Biology Organization | All Rights Reserved 0261-4189/08
www.embojournal.org

THE EMBO JOURNAL

# Spatial and temporal role of the apelin/APJ system in the caliber size regulation of blood vessels during angiogenesis

Hiroyasu Kidoya[1], Masaya Ueno[1], Yoshihiro Yamada[1], Naoki Mochizuki[2], Mitsugu Nakata[3], Takashi Yano[3], Ryo Fujii[4] and Nobuyuki Takakura[1,*]

[1]Department of Signal Transduction, Research Institute for Microbial Diseases, Osaka University, Suita, Osaka, Japan, [2]Department of Structural Analysis, National Cardiovascular Center Research Institute, Suita, Osaka, Japan, [3]Pharmaceutical Research Laboratories 1, Pharmaceutical Research Division, Takeda Pharmaceutical Company Limited, Yodogawa, Osaka, Japan and [4]Frontier Research Laboratories, Pharmaceutical Research Division, Takeda Pharmaceutical Company Limited, Tsukuba-shi, Ibaraki, Japan

**Blood vessels change their caliber to adapt to the demands of tissues or organs for oxygen and nutrients. This event is mainly organized at the capillary level and requires a size-sensing mechanism. However, the molecular regulatory mechanism involved in caliber size modification in blood vessels is not clear. Here we show that apelin, a protein secreted from endothelial cells under the activation of Tie2 receptor tyrosine kinase on endothelial cells, plays a role in the regulation of caliber size of blood vessel through its cognate receptor APJ, which is expressed on endothelial cells. During early embryogenesis, APJ is expressed on endothelial cells of the new blood vessels sprouted from the dorsal aorta, but not on pre-existing endothelial cells of the dorsal aorta. Apelin-deficient mice showed narrow blood vessels in intersomitic vessels during embryogenesis. Apelin enhanced endothelial cell proliferation in the presence of vascular endothelial growth factor and promoted cell-to-cell aggregation. These results indicated that the apelin/APJ system is involved in the regulation of blood vessel diameter during angiogenesis.**

*The EMBO Journal* (2008) **27**, 522–534. doi:10.1038/sj.emboj.7601982; Published online 17 January 2008
*Subject Categories*: development
*Keywords*: angiogenesis; angiopoietin-1; apelin; APJ; lumen size

## Introduction

The vascular system of vertebrates has a highly organized and hierarchical structure, ranging from large blood vessels down to finely sized capillaries. The intraluminal cavity of blood vessels is lined almost exclusively with endothelial cells (ECs). The formation of blood vessels is initiated by the assembly and tube formation of ECs, or EC progenitors. This process is termed vasculogenesis and is followed by angiogenesis, which results in the emergence of new vessels through sprouting and elongation from, or the remodelling of, pre-existing vessels (Risau, 1997).

Many genes involved in these processes have been isolated and their roles in the specification of vascular lineage from mesodermal cells and vascular morphogenesis have been analysed (Wang *et al*, 1998; Adams *et al*, 1999; Gale and Yancopoulos, 1999; Oettgen, 2001; Zhong *et al*, 2001; Carmeliet, 2003; Gerhardt and Betsholtz, 2003; Simon, 2004). Among many molecules, vascular endothelial growth factors (VEGFs) and their cognate receptors (VEGFRs) play central roles in the differentiation (arterial), proliferation, migration and survival of ECs in physiological and pathological conditions (Ferrara *et al*, 2003). Based on the diverse functions of VEGFs in blood vessel formation, the VEGF/VEGFR system has proved effective in the clinical management of cancer patients by negatively regulating angiogenesis (Ferrara and Alitalo, 1999; Jain, 2005). Therefore, these results indicate the importance of developmental studies for understanding blood vessel formation.

In the maturation process involved in blood vessel formation, the ECs, which form the tube, recruit supporting mural cells (MCs) such as periendothelial cells (pericytes) or vascular smooth muscle cells, by releasing platelet-derived growth factor (PDGF)-BB (Lindahl *et al*, 1997). MCs subsequently adhere to ECs resulting in the formation of a structurally stable blood vessel. It has been proposed that this cell adhesion between ECs and MCs is induced when angiopoietin 1 (Ang1), produced from MCs, stimulates Tie2, a receptor tyrosine kinase on ECs (Dumont *et al*, 1994; Sato *et al*, 1995; Suri *et al*, 1996).

During angiogenesis, blood vessels need to be able to adjust their caliber, in order to allow them to respond adequately to the changes in demand for oxygen and nutrients made by the organs and tissues. This caliber adjustment is involved in the maturation process during angiogenesis; however, the molecular mechanism involved in the determination of blood vessel size has not been elucidated. A potent regulator of the enlargement of blood vessel caliber is the Ang1/Tie2 system, because transgenic overexpression of Ang1 in the keratinocyte-induced enlarged blood vessels in the dermis (Suri *et al*, 1998) and administration of a potent Ang1 variant were also reported to induce enlargement of blood vessels (Cho *et al*, 2005; Thurston *et al*, 2005). Therefore, the analysis of the precise molecular mechanism of how the Ang1/Tie2 system induces enlargement of blood vessels would allow us to understand the process of determination of blood vessel size during angiogenesis.

In this report, by the analysis of downstream signalling of Ang1/Tie2 in ECs, we found that apelin, a recently isolated bioactive peptide from bovine gastric extract working as a

*Corresponding author. Department of Signal Transduction, Research Institute for Microbial Diseases, Osaka University, 3-1 Yamadaoka, Suita, Osaka 565-0871, Japan. Tel.: +81 6 6879 8316; Fax: +81 6 6879 8314; E-mail: ntakaku@biken.osaka-u.ac.jp

**Received: 19 April 2007; accepted: 18 December 2007; published online: 17 January 2008**

ligand for APJ, is upregulated by Ang1 stimulation of human umbilical vein endothelial cells (HUVECs). A sequence of apelin cDNA encodes a protein of 77 amino acids, which can generate two active polypeptides: the long (42–77) and the short (65–77) forms of apelin (Tatemoto *et al*, 1998; Kawamata *et al*, 2001; Masri *et al*, 2005). Both forms activate APJ.

APJ is a G protein-coupled receptor, which has been reported to be expressed in the cardiovascular and central nervous systems (O'Dowd *et al*, 1993; Devic *et al*, 1999). In brain tissues, APJ expression is observed in neurons (Edinger *et al*, 1998) as well as in oligodendrocytes and astrocytes (Croitoru-Lamoury *et al*, 2003). In the brain, the apelin/APJ system plays a role in maintaining body fluid homeostasis and regulating the release of vasopressin from the hypothalamus (De Mota *et al*, 2004). In the cardiovascular system, APJ is expressed in an endothelial lineage in various species such as amphibian, mouse and human (Devic *et al*, 1996, 1999; Katugampola *et al*, 2001). In the mouse and human, the expression of the receptor has also been detected by immunocytochemistry in vascular smooth muscle cells and cardiomyocytes (Kleinz and Davenport, 2004). Apelin/APJ function in cardiomyocytes is thought to be associated with a very strong inotropic activity (Szokodi *et al*, 2002; Ashley *et al*, 2005). The function of apelin/APJ in EC lineage is reported to be associated with the hypotensive activity of apelin (Ishida *et al*, 2004), as the activation of APJ leads to nitric oxide (NO) production by the ECs (Tatemoto *et al*, 2001), and this possibly plays a role in the relaxation of smooth muscle cells.

Using the morpholino antisense oligonucleotide, requisite roles of the apelin/APJ system have been reported in the cardiovascular system of *Xenopus laevis* (Cox *et al*, 2006; Inui *et al*, 2006) and zebrafish (Scott *et al*, 2007). *Xenopus apelin* (*Xapelin*) was detected in the region around the presumptive blood vessels during early embryogenesis and overlapped with the expression of *Xmsr*, the *Xenopus* homolog of *APJ*. Overexpression of *Xapelin* disorganized the expression of the endothelial precursor cell marker *XIFli* at the neurula stage. Knockdown of *Xapelin* or Xmsr induced abnormal heart morphology and attenuated the expression of *Tie2*, resulting in the disruption of blood vessel formation in the posterior cardinal vein, intersomitic vessels (ISVs) and vitelline vessels. By contrast, apelin protein has been shown to induce angiogenesis in the chicken chorioallantoic membrane assay (Cox *et al*, 2006). Although the involvement of apelin/APJ in angiogenesis and the regulation of proliferation of ECs has been suggested, the precise function of apelin/APJ in the morphology of blood vessels in mammals is not clear.

Here, using various *in vitro* and *in vivo* assays, we show that apelin induces enlargement of blood vessels. Moreover, the physiological function of apelin has been studied through the generation of apelin-mutant mice and the relationship of Ang1/Tie2 signalling to apelin has been studied by mating apelin-mutant mice with Ang1 transgenic mice. Finally, using the para-aortic splanchnopleural mesoderm (P-Sp) organ culture system that mimics *in vivo* vasculogenesis and angiogenesis and various *in vitro* HUVEC culture systems, we have studied how apelin regulates the enlargement of blood vessels.

## Results

### *Ang1 induces apelin expression on ECs*

To elucidate the molecular mechanism by which Tie2 regulates the caliber change of blood vessels from small to larger ones, and in order to isolate the genes encoding proteins that are involved in caliber change and specifically expressed in HUVECs stimulated by Ang1, we constructed a subtraction library from HUVECs with Tie2 stimulated by Ang1 as a tester, and HUVECs with no stimulation of Tie2 as the driver (Figure 1A). One of these isolated cDNA clones was the human gene encoding apelin (Figure 1B–D). Real-time polymerase chain reaction (PCR) analysis revealed that apelin mRNA was potently increased in HUVECs after stimulation by Ang1 in a time-dependent manner (Figure 1B) and we confirmed that the expression of apelin protein was markedly upregulated on HUVECs stimulated by Ang1 (Figure 1C). Moreover, the dose-dependent effect of Ang1 on apelin production from HUVECs was confirmed by enzyme immunoassay, using the culture supernatant of HUVECs (Figure 1D).

In order to confirm further the upregulation of apelin in ECs *in vivo*, we analysed apelin expression in the dermis of Ang1 transgenic (Ang1Tg) mice, in which Ang1 was overexpressed in the keratinocytes under the transcriptional control of K14 promoter (Suri *et al*, 1998). As shown in Figure 1E, apelin expression on ECs in the dermis at postnatal day 7 was increased in Ang1Tg mice compared to that in wild-type (WT) mice. We confirmed the overexpression of apelin mRNA in Ang1Tg mice by quantitative real-time RT–PCR using ECs fractionated from the dermis by a cell sorter (Figure 1F). As it is well known that Ang1 is involved in angiogenesis, next we observed the effect of other proangiogenic molecules on the expression of apelin on ECs. bFGF induced apelin expression on HUVECs; however, VEGF, PDGF-BB or EGF did not affect apelin expression (Supplementary Figure 1A and B).

### *Apelin with VEGF induces proliferation of ECs*

With respect to the enlargement of blood vessels, it seems likely that apelin causes the proliferation of ECs. To test this ability, firstly we studied the proliferation of ECs using HUVECs. As shown in Figure 2A, apelin was not effective in inducing proliferation of HUVECs. However, upon stimulation with VEGF, the expression level of APJ was upregulated in HUVECs, at both the mRNA and protein levels (Figure 2B–D and Supplementary Figure 2). Cell surface expression of APJ on HUVECs was confirmed by both cell surface biotinylation experiment (Figure 2D) and confocal laser scanning analysis (Supplementary Figure 2). Consistent with this result, VEGF-induced proliferation of HUVECs was enhanced by the addition of apelin in a dose-dependent manner (Figure 2A). Among proangiogenic cytokines, such as Ang1, EGF, bFGF, PDGF-BB and VEGF, only VEGF induced APJ expression on HUVECs (Figure 2B–D and Supplementary Figure 1C and D).

These results suggested that APJ is expressed and affects ECs during angiogenesis in which VEGF levels are upregulated. Next we observed the proliferation of primary ECs from the culture of the AGM region (aorta–gonad–mesonephros region followed by P-Sp region at embryonic day (E) 10.5 to E11.5) in which angiogenesis was actively taking place. APJ was highly expressed in the AGM region compared to other tissues, such as E10.5 yolk sac, head region and heart, and adult heart (Figure 3A). Furthermore, APJ was expressed strongly in $CD45^{-}CD31^{+}$ ECs from the AGM region compared to those from E10.5 heart and adult heart. Although ECs in E10.5 yolk sac and head region expressed APJ, the

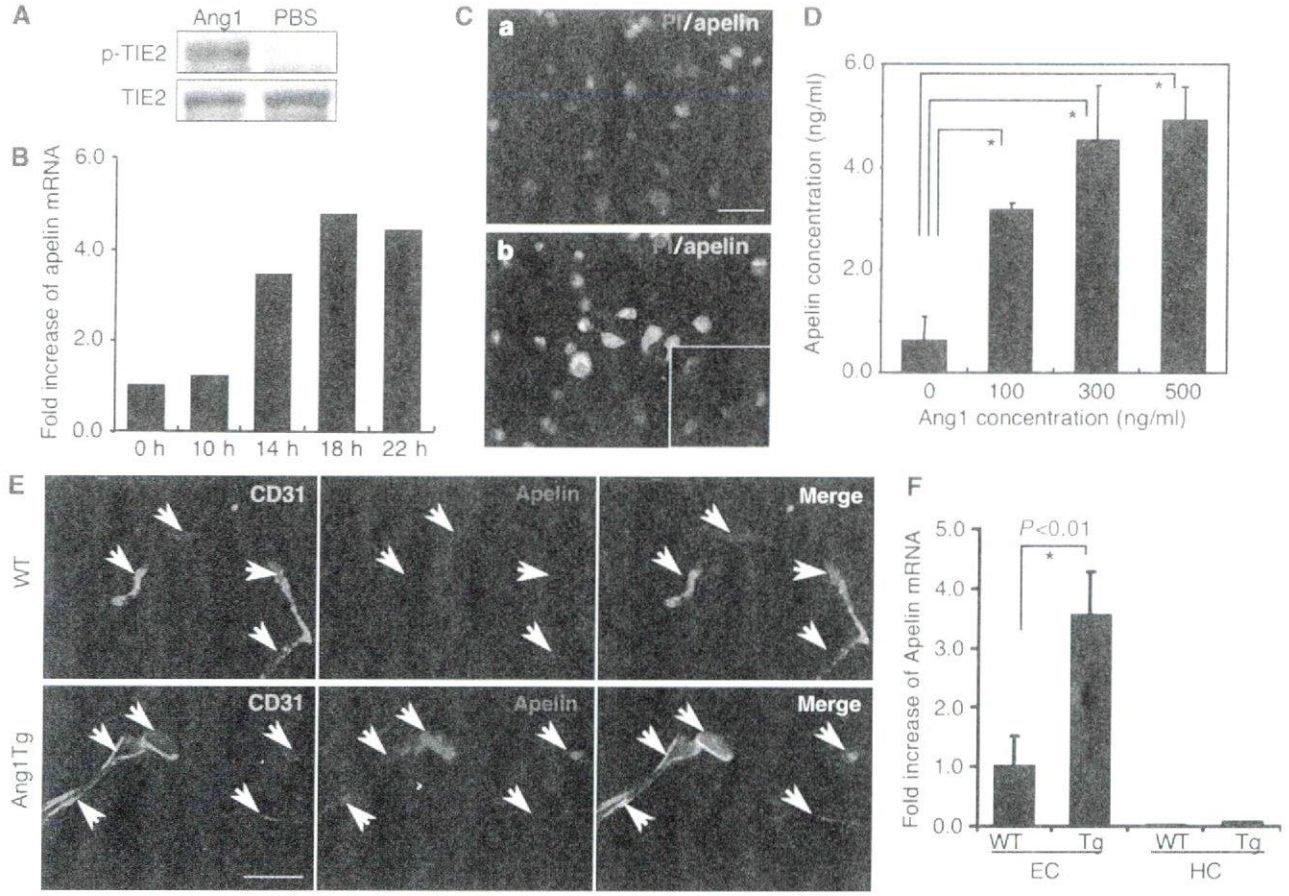


**Figure 1** Ang1 stimulation induces apelin expression in ECs *in vitro* and *in vivo*. (**A**) Tie2 phosphorylation on HUVECs by Ang1 in our system. HUVECs, serum-starved for 2 h, were either treated or not treated with 500 ng/ml Ang1 for 10 min. Phosphorylation was studied by immunoblotting using phosphospecific antibody (p-Tie2). (**B**) Quantitative real-time RT–PCR analysis of apelin mRNA in HUVECs. Total RNA was extracted from HUVECs that had been stimulated with Ang1 for 0–22 h. Results are shown as fold increase in comparison with basal levels of HUVECs (0 h). (**C**) Immunocytochemical analysis of apelin expression in HUVECs, non-stimulated (a) and stimulated (b) by Ang1 (500 ng/ml) for 20 h. Cells were stained with anti-apelin mAb (green). The inset in (b) shows HUVECs stained with secondary antibody as a negative control. Nuclei were stained with propidium iodide (PI; red). Scale bar indicates 50 μm. (**D**) Quantitative enzyme immunoassay of apelin production from HUVECs stimulated by various doses of Ang1. $^{*}P<0.001$ ($n=3$). (**E**) Immunochemical detection of apelin peptide in the dermis. Sections of skin from WT and Ang1Tg neonatal mice were stained with anti-CD31 (green) and anti-apelin (red) mAb. Arrows indicate CD31$^{+}$ blood vessels. Scale bar indicates 30 μm. (**F**) Quantitative real-time RT–PCR analysis of apelin mRNA in ECs and hematopoietic cells (HCs) of Ang1Tg mice. RNA was prepared from sorted CD31$^{+}$CD45$^{-}$ ECs or CD31$^{-}$CD45$^{+}$ HCs from the dermis of WT or Ang1Tg neonatal mouse skin. $^{*}P<0.01$ ($n=3$).

expression level was weaker than that in the AGM region. When cells from the AGM region were cultured on apelin-expressing OP9 cells (Figure 3B), proliferation of CD45$^{-}$CD31$^{+}$ was increased compared with that on control OP9 cells and this proliferation by apelin was abrogated by the addition of anti-apelin blocking antibody (Figure 3C and D), suggesting that this action of proliferation by apelin is specific to the apelin/APJ system. Moreover, as APJ expression was weaker in ECs from adult heart (Figure 3A) or adult liver (data not shown) than in those from the AGM region, apelin did not induce proliferation of ECs in such adult tissues compared to those in the AGM region (Supplementary Figure 3).

### *Apelin induces the assembly of ECs*

Although the proliferation of ECs is one of the factors involved in the construction of larger vessels, it is not the only one. The assembly or aggregation of ECs or endothelial progenitors, resulting in abundant cell-to-cell contact, is also necessary for the induction of a caliber change of blood vessels into larger ones. Therefore, next we tested the ability of apelin to regulate cell-to-cell contact. When cells from the AGM region were put on OP9 feeder cells, the control OP9 cells induced a cord-like structure of ECs, in contrast to the OP9 cells expressing apelin, which induced a sheet-like layer of ECs in abundance (Figure 4A and C). When cell-to-cell contact was observed using anti-VE-cadherin or -claudin5 antibodies, we confirmed that the sheet-like structure was composed of ECs connected with the junctional proteins, VE-cadherin (Figure 4B) or claudin5 (Supplementary Figure 4). Moreover, the addition of anti-apelin monoclonal antibody (mAb) inhibited the sheet-like layer formation of ECs induced by apelin (Figure 4B and Supplementary Figure 4). This sheet-like structure was already observed in the early stage of this culture (Figure 4C), suggesting that cell aggregation was initiated when ECs were seeded on OP9 cells expressing apelin.

Among many adhesion molecules tested, we found that the expression of the junctional protein, claudin5, was significantly induced by apelin on HUVECs, while that of VE-cadherin was only slightly induced, at both the mRNA

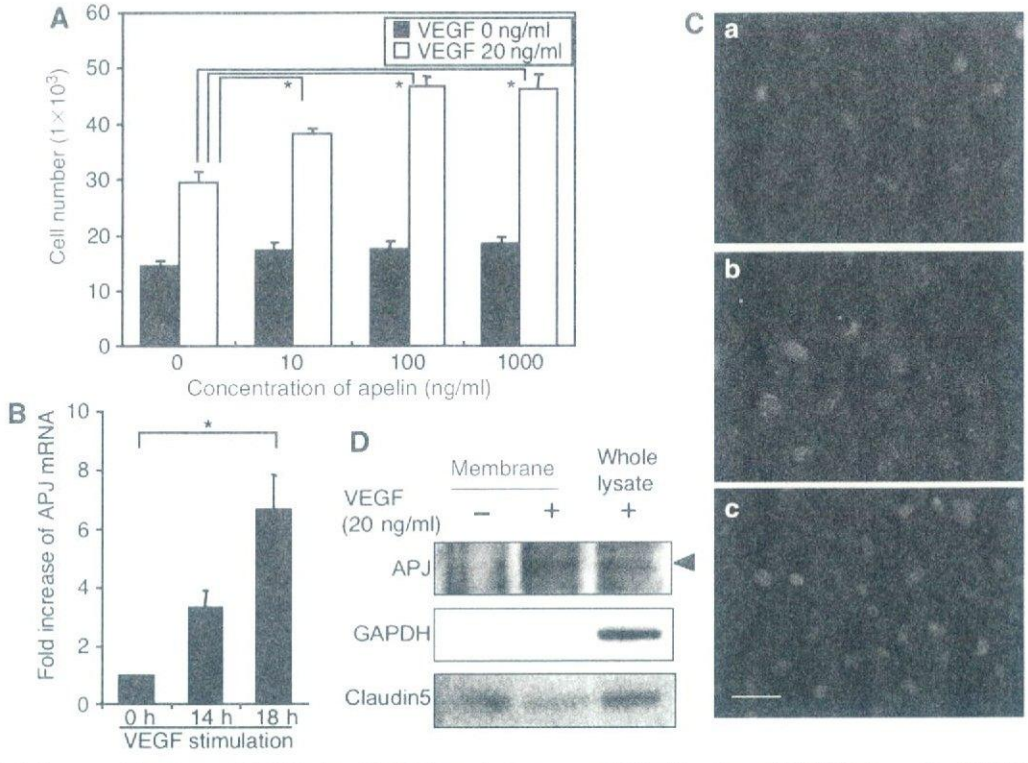


**Figure 2** Apelin induces proliferation of HUVECs in a VEGF-dependent manner. (**A**) Proliferation of HUVECs by apelin. HUVECs ($5 \times 10^3$) were cultured with apelin (0–1000 ng/ml) in the presence or absence of VEGF (20 ng/ml) for 48 h and the number of cells was counted. $^*P<0.001$ ($n=3$). (**B**) Quantitative real-time RT–PCR analysis of the induction of APJ expression by VEGF in HUVECs. HUVECs were stimulated with VEGF (10 ng/ml) for 0–18 h. Results are shown as fold increase in expression in comparison with levels in stimulated HUVECs at 0 h. $^*P<0.001$ ($n=3$). (**C**) APJ expression on HUVECs. HUVECs were cultured in the absence (a) or presence (b, c) of VEGF (20 ng/ml) for 24 h and stained with anti-APJ antibody (green) (a, b). (c) Cells stained with a secondary antibody alone as a negative control. Nuclei were stained with propidium iodide (red). Scale bar indicates 50 μm. (**D**) Western blot analysis of cell surface APJ expression on HUVECs that had been stimulated with VEGF (20 ng/ml) for 24 h. The purity of cell membrane protein was confirmed by the lack of intracellular protein GAPDH expression. Claudin5 expression was analysed for the experimental control of another cell surface protein. Note that the expression of a 60 kDa APJ protein was increased in HUVECs in the presence of VEGF.

and protein levels (Supplementary Figure 5). *In vitro* sheet-like formation of ECs and upregulation of cell-to-cell adhesion molecules by apelin indicated the involvement of the apelin/APJ system in the assembly of ECs. Next, we performed the cord formation assay of HUVECs on Matrigel in the presence or absence of apelin (Figure 5A). After 20 h of culture of HUVECs on Matrigel, they formed a cord-like structure in the absence of apelin (Figure 5Aa). However, in the presence of apelin, the HUVECs formed an enlarged cord-like structure (Figure 5Abd). In this assay, by using confocal laser scanning analysis, we confirmed that enlargement of this cord-like structure was induced by cell aggregation, but not by cell spreading (Supplementary Figure 6). This enlargement was completely blocked by anti-VE-cadherin blocking antibody (Figure 5Acd), suggesting that the enlarged cord-like formation induced by apelin was initiated by cell-to-cell contact. Moreover, in the spheroid assay (Korff and Augustin, 1998), HUVECs formed large spheroids in the presence of apelin (Figure 5B) and this action was abrogated by anti-apelin antibody. Therefore, these results strongly support the notion that the apelin/APJ system induces EC-to-EC assembly.

### *APJ expression in ECs during early embryogenesis*

As APJ expression was observed in ECs during early embryogenesis (Figure 3), we studied which vessels expressed APJ in mouse embryos. At E8.5, cells committed into the endothelial lineage formed the dorsal aorta (DA), from which ECs started to sprout. As observed in Figure 6A, APJ expression was observed in those ECs that had sprouted from the DA but not in those that were forming the DA. At E9.5, APJ expression was observed in the migrating end region of ISVs sprouting from the DA (Figure 6B). Besides the expression of APJ in the ISVs, weak APJ expression was observed in the somites. These expression profiles were not very different from the results obtained by *in situ* hybridization analysis, as reported previously (Devic *et al*, 1999). In another area of the E9.5 embryo, we found that the anterior cardinal vein (ACV) expressed APJ. However, when compared to CD31 expression in ECs, APJ-positive ECs were observed in the migrating end of the ACV, but not in the base (Supplementary Figure 7). These expression profiles suggest that the apelin/APJ system may be associated with angiogenesis but not with vasculogenesis. Moreover, when apelin expression was observed in the somite region at E9.5, we found that apelin protein was detected in ISV (Supplementary Figure 8), suggesting that the apelin/APJ system may be associated with the formation of ISV.

### *Narrow blood vessels are induced in apelin-mutant mice*

In order to understand the physiological function of apelin, we generated apelin-mutant mice (Supplementary Figure 9)

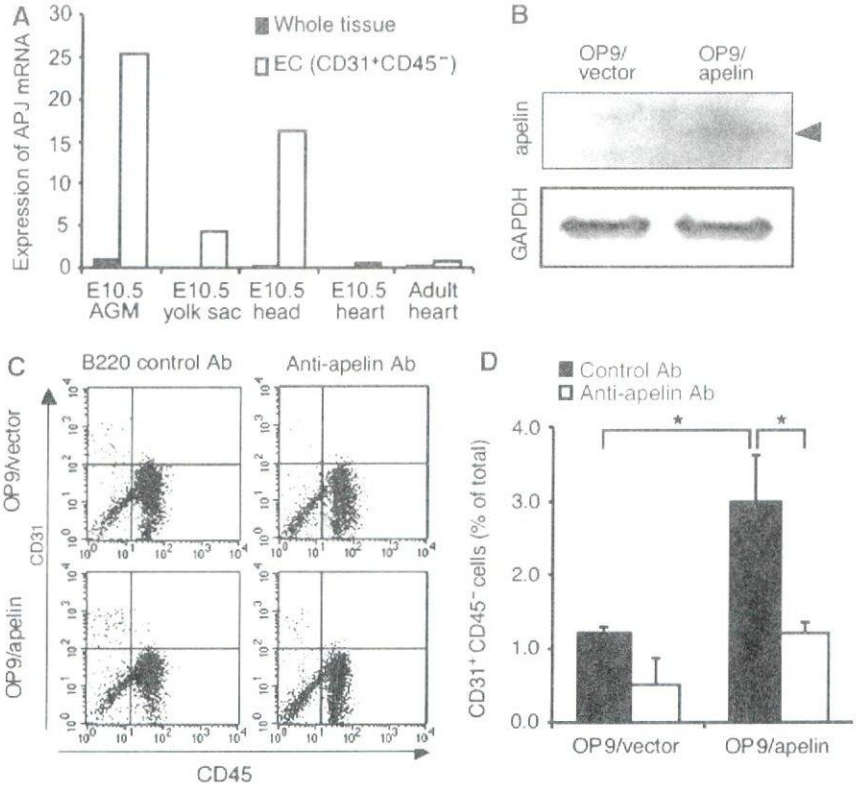


**Figure 3** ECs from the AGM region express APJ and are induced to proliferate by apelin. (**A**) Quantitative real-time RT–PCR analysis of APJ expression in various tissues, as indicated. RNA from whole tissue, or CD45$^-$CD31$^+$ ECs sorted from various tissues, was evaluated for the expression of APJ. (**B**) Western blot analysis of apelin expression on OP9 cells induced by mock vector (OP9/vector) or apelin expression vector (OP9/apelin). An 8 kDa apelin protein was detected in OP9/apelin. GAPDH was used for the internal control. (**C**) Apelin-induced proliferation of ECs from E10.5 AGM region. Cells from the AGM region were cultured for 7 days, on an OP9/vector or OP9/apelin, in the presence or absence of anti-apelin or control B220 mAb. AGM cells harvested from cultures were stained with anti-CD31 and -CD45 mAbs and analysed by FACS. (**D**) Quantitative evaluation of the percentage of CD31$^+$CD45$^-$ vascular ECs cultured as described in (C). $^*P<0.001$ ($n=5$).

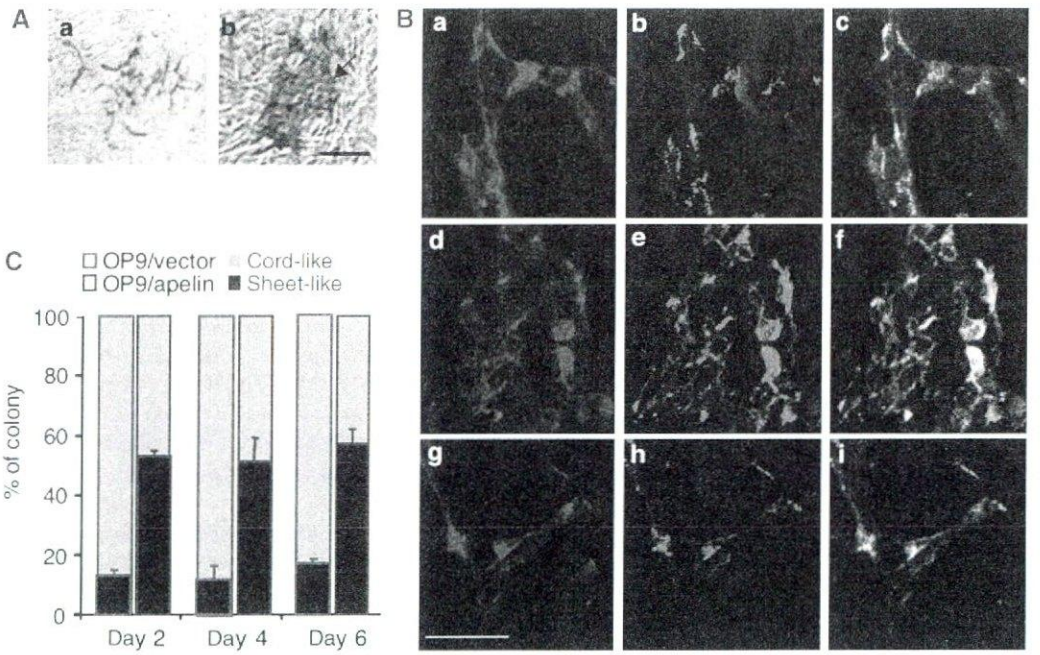


**Figure 4** Endothelial sheet formation by apelin. (**A**) Cells from E11.5 AGM region were cocultured with an OP9/vector (a) or OP9/apelin (b) for 2–6 days, and CD31 immunostaining was performed. The arrow indicates the aggregated EC sheet. Scale bar indicates 100 μm. (**B**) Cells from E11.5 AGM region were cocultured for 6 days with an OP9/vector (a–c), OP9/apelin in the presence of B220 control antibody (d–f) or OP9/apelin in the presence of anti-apelin blocking antibody (g–i). ECs on OP9 cells were stained with anti-CD31 (a, d, g) and anti-VE-cadherin (b, e, h) antibodies. (c, f, i) Merged images of (a) and (b), (d) and (e), or (g) and (h), respectively. Scale bar indicates 50 μm. (**C**) The proportion of sheet-like or cord-like structures of ECs on OP9/apelin or OP9/vector stromal cells ($n=3$).

 

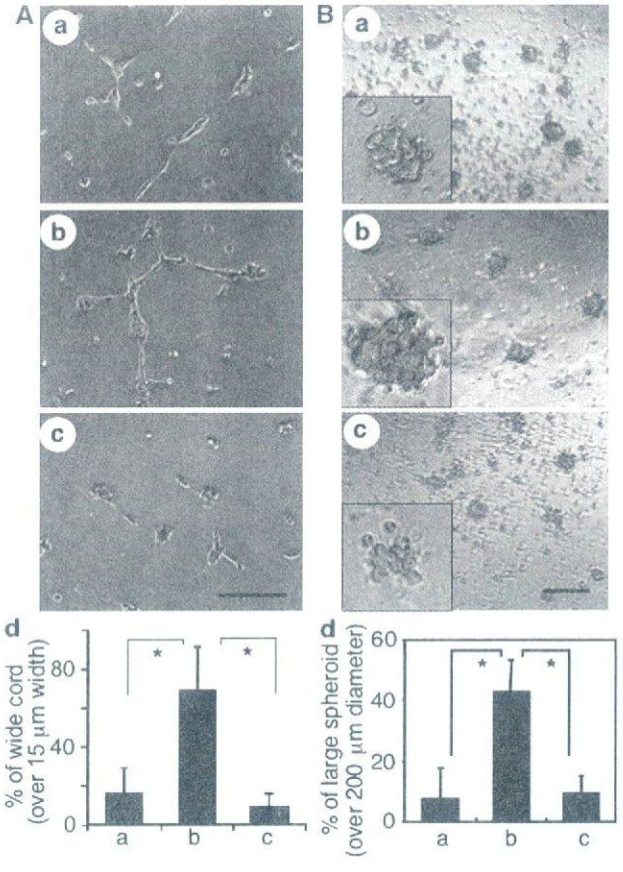


**Figure 5** Morphological change of HUVECs stimulated with apelin. (**A**) Cord formation analysis of HUVECs cultured on Matrigel. HUVECs were cultured in the presence of VEGF (20 ng/ml) for 20 h, harvested, transferred onto Matrigel and cultured in the absence (a) or presence of apelin (b, c) for 10 h. Anti-VE-cadherin antibody (c) or control anti-B220 mAb (b) was added. Scale bar indicates 200 μm. (d) Quantitative evaluation of the width of the cord-like structure observed in the various culture conditions (a: control; b: apelin + anti-B220 mAb; c: apelin + anti- VE-cadherin antibody) described above. The percentage of wide cord (width >15 μm) among the total cord-like structure was calculated. $^*P<0.01$ ($n=3$). (**B**) HUVEC spheroid assay. HUVECs stimulated with VEGF for 24 h were harvested and cultured on nonadhesive dishes in the absence (a) or presence of apelin (b, c) for 10 h. Anti-apelin antibody (c) or control anti-B220 mAb (b) was added. Scale bar indicates 500 μm. The inset in each panel shows higher magnified representative spheroid under each condition. (d) Quantitative evaluation of the size of spheroid observed in the various culture conditions (a: control; b: apelin; c: apelin + anti-apelin antibody) described above. The percentage of large spheroid (diameter >200 μm) among the total spheroid was calculated. $^*P<0.01$ ($n=3$).

and observed blood vessel formation. Mice heterozygous for apelin were intercrossed and their offspring were obtained. The frequency of mutant homozygotes obtained in heterozygote intercrosses was close to the expected 25%, suggesting that apelin-deficient mice are not embryonically lethal. Although a small population of apelin-mutant mice lacked eyes and lost a great deal of weight, for reasons that have not been determined as yet, generally, the mutant animals appeared healthy as adults. Crosses between homozygous apelin-mutant animals were also fertile, indicating that implantation and embryonic development can apparently occur normally even when apelin is absent from both the embryo and the mother.

As apelin deficiency in *Xenopus* leads to severe disorganized blood vessel formation (Cox *et al*, 2006; Inui *et al*, 2006) and might induce embryonic lethality, it is possible that other unknown molecules compensate and rescue apelin deficiency in mammals. Before a compensatory effect was investigated, we studied the ISV at E9.5 (Figure 7A–C and Supplementary Figure 10), because we found that APJ expression was clearly observed in vessels sprouted from the DA into the somite (Figure 6). The results showed that body size and number of somites were equivalent between WT and apelin-mutant embryos at E9.5, but that the caliber of ISVs was narrower in apelin-deficient embryos compared with WT embryos. The expression of APJ was observed in all ECs of ISV sprouted from the DA, ranging from the base region of the sprout to the migrating end at E8.5; the expression had disappeared in the base region near the DA at E9.5 (Figure 6). This expression pattern in the phenotype of apelin-deficient embryos suggests that APJ expression is regulated by VEGF or other unknown molecules in ECs at the migrating end, in order to regulate the caliber size of blood vessels.

General Ang1 administration has been reported to induce enhancement of blood vessel formation in the trachea of adult mice (Cho *et al*, 2005). This indicates that tracheal blood vessels are active in angiogenesis in adulthood and it is possible that apelin deficiency affects blood vessel formation in this region. As expected, the blood vessels observed in the trachea of apelin-deficient mice were narrower than those in WT mice and, in addition, the capillary density was lower (Figure 8). Moreover, the blood vessels observed in the dermis (Figure 9 and Supplementary Figure 11) and heart (data not shown) of apelin-deficient mice were narrower than those in WT mice.

Through the use of the *in situ* hybridization method of APJ expression, it has been reported that APJ is not expressed on larger vessels such as DA, except for the posterior cardinal vein during early embryogenesis at around E9.5 (Devic *et al*, 1999). This result is consistent with our immunohistochemical analysis. The caliber sizes of the aorta and vena cava, and their major branches such as brachiocephalic, subclavian and common iliac arteries and veins, were not affected by the lack of apelin (data not shown). Therefore, this suggests that apelin may not be involved in the regulation of caliber size of larger vessels. Moreover, although apelin deficiency in *Xenopus* led to severely disorganized blood vessels in the vitelline (Cox *et al*, 2006; Inui *et al*, 2006), it did not affect the remodelling of blood vessels in the yolk sac (Supplementary Figure 12).

In order to analyse precisely the function of the exogenous apelin in the *in vitro* culture system, it was necessary to exclude from the analysis any confounding effects of the contaminating apelin from the culture serum, as well as the endogenous apelin produced from cultured cells. In order to achieve this, we tried to culture the aorta ring from apelin-deficient mice under quite low serum-containing conditions (Figure 7D and E). Although VEGF induced sprouting of ECs from the aorta, apelin on its own did not. However, the caliber size of VEGF-induced sprouts was enlarged upon the addition of apelin. Most of the sprouts induced by VEGF plus apelin contained large luminal cavities (data not shown). Therefore, we confirmed that apelin regulates caliber change in angiogenesis and this effect is induced in the

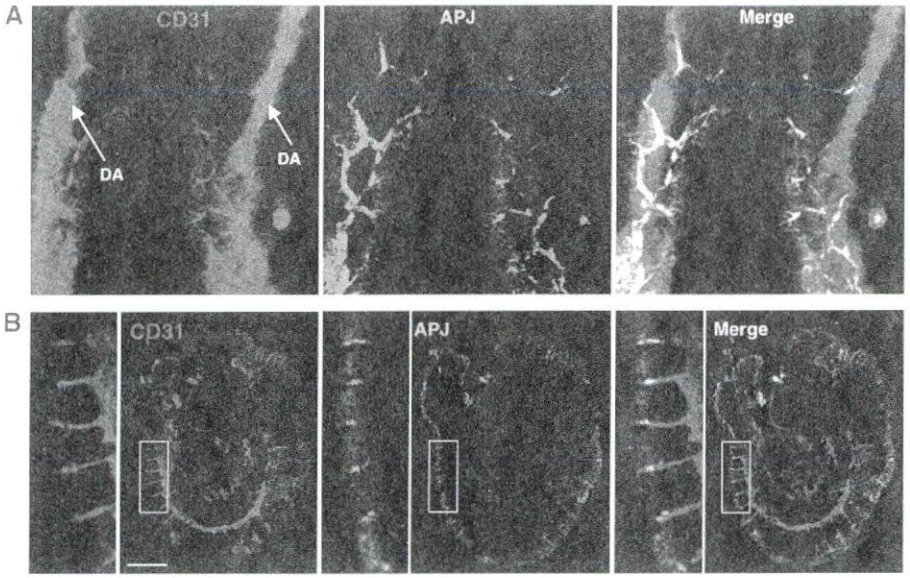


**Figure 6** Expression of APJ in embryo. (**A**) Whole-mount staining of E8.5 mouse embryo with anti-CD31 (red) and anti-APJ (green) antibodies. (**B**) Staining of E9.5 mouse embryo section with anti-CD31 (red) and anti-APJ (green) Abs. The left panel shows high-power view of the area indicated by the box. Note that the DA stained by anti-CD31 Ab did not express APJ and APJ expressed on ECs sprouting from DA. Scale bar indicates 500 μm.

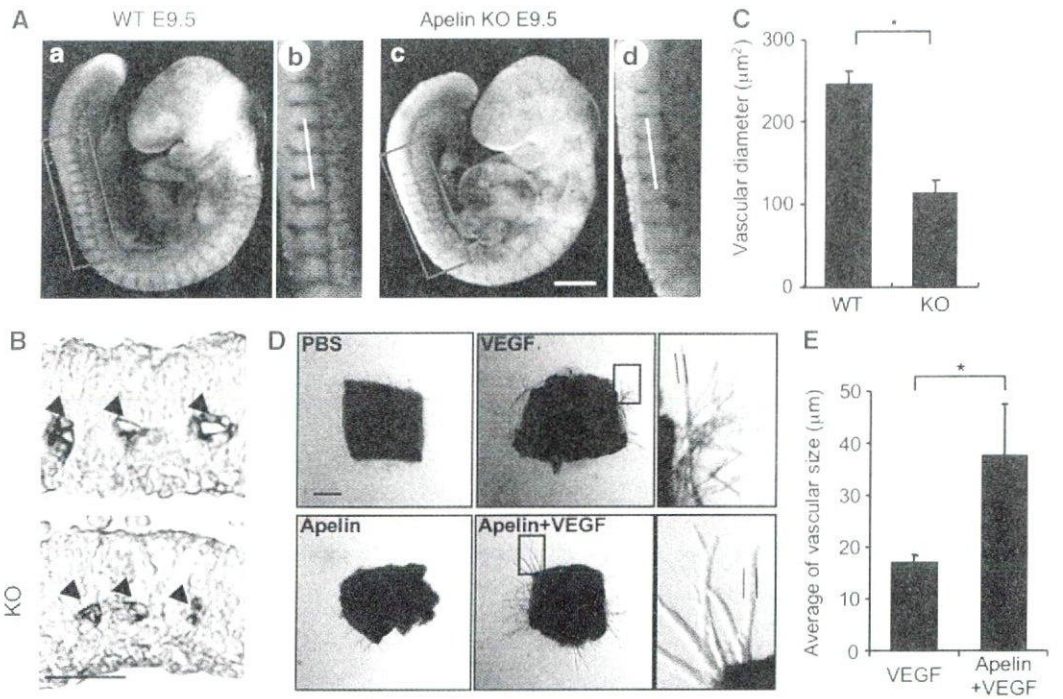


**Figure 7** Defect of the enlargement in blood vessel caliber in apelin-deficient mice. (**A**) Whole-mount immunohistostaining of WT (a, b) and apelin-deficient (c, d) embryos at E9.5 with anti-CD31 Ab. (b) and (d) are higher magnifications of the areas indicated by the box in (a) and (c), respectively. Scale bar indicates 300 μm. (**B**) Sections containing ISVs (arrowheads) from WT and apelin-deficient (KO) embryos at E9.5 were stained with anti-CD31 antibody. The level of the sectioning position is indicated by a white bar in (b) and (d). Scale bar indicates 30 μm. (**C**) Quantitative evaluation of the vascular diameter of intersomitic blood vessels from apelin-deficient (KO) versus WT mice. $^*P<0.001$ (30 vessels from 5 embryos were examined). Details of the measurement of vascular diameter are shown in Supplementary Figure 7. (**D**) Representative pictures of microvessels sprouted from aortic ring using apelin-deficient mice. Aortic ring was cultured in the presence or absence of VEGF (10 ng/ml) or apelin (100 ng/ml). PBS was used as a negative control. Pictures in the right panel show a high-power view of the area indicated by the box, respectively. Scale bar indicates 300 μm. (**E**) Quantitative evaluation of the vascular size of sprouted microvessels from the aortic ring cultured as described in (D). Vascular size was measured as the length between two parallel lines as indicated in (D). $^*P<0.003$ ($n=30$).

absence of blood flow. It is known that blood flux regulates vessel size (Koller and Huang, 1999). Therefore, it is possible that shear stress may induce apelin expression in ECs. However, the results were contrary to our expectation. *In vitro* shear stress on HUVECs attenuated apelin mRNA expression in HUVECs (Supplementary Figure 13).

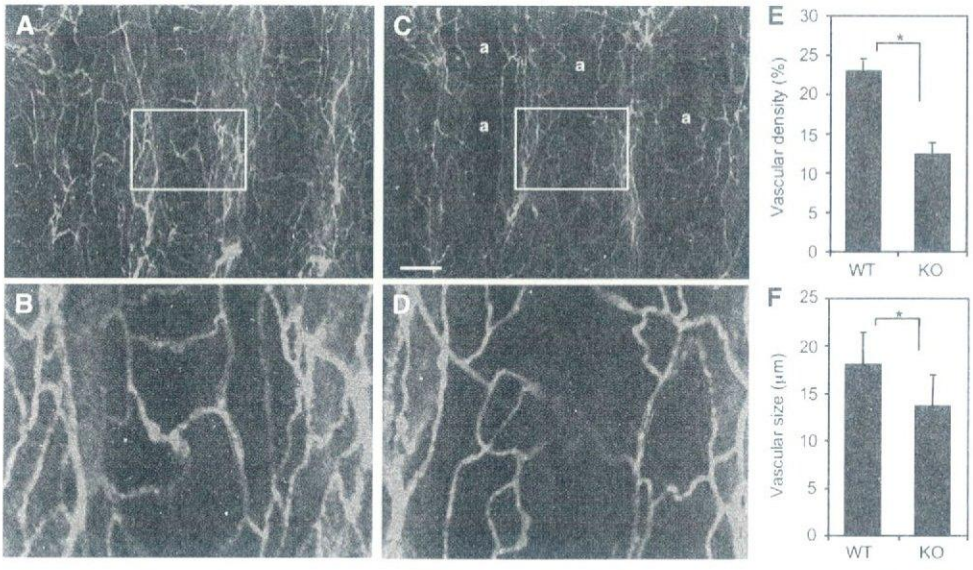


**Figure 8** Lectin staining of tracheal blood vessels. (A–D) Comparison of tracheal blood vessels in 8-week-old WT (**A**, **B**) and apelin-deficient (**C**, **D**) mice stained by intravenous injection of fluorescein-labelled lectin. a in (C) means avascular area. (B) and (D) show a high-power view of the area indicated by the box in (A) and (C), respectively. Scale bar in (C) indicates 200 μm (A, C) and 60 μm (B, D). (**E**) Quantitative evaluation of vascular density from apelin-deficient (KO) versus WT mice. $^*P<0.001$. Vascular density from 10 random fields was counted. (**F**) Quantitative evaluation of vascular size of blood vessels in the trachea from apelin-deficient (KO) versus WT mice. Vascular size was measured as the length between two parallel red lines as indicated in (B) and (D). $^*P<0.001$ (100 vessels from 3 mice were examined).

### *Role of apelin in Ang1-induced enlargement of capillary size*

We isolated apelin from ECs under the activation of Tie2 by Ang1. Next, using apelin-deficient mice, we observed whether Ang1-induced enlargement of blood vessels is suppressed in the absence of apelin. In this experiment, we mated apelin-deficient mice with Ang1Tg mice and observed the caliber size of the capillaries in the dermis (Figure 9).

In apelin-deficient mice, the caliber size of the capillary in the dermis was narrower compared with that in WT mice (Figure 9A and B and Supplementary Figure 11). We confirmed that CD31-positive cells are from blood vessels but not from lymphatic vessels, by double staining with LYVE1, a specific marker for lymphatic ECs (Supplementary Figure 11). As previously reported (Suri *et al*, 1998), Ang1Tg mice showed enlarged capillary formation in the dermis, but this effect of Ang1 was abolished by the lack of apelin (Figure 9A and B). However, apelin deficiency did not completely suppress Ang1-induced enlargement of blood vessels, suggesting that other molecules upregulated by Tie2 activation might be involved in the caliber size determination of capillaries *in vivo*. On the other hand, the generation of extremely enlarged blood vessels, with a caliber size of more than $10^4\,\mu m^2$, observed in Ang1Tg mice, was completely suppressed in the absence of apelin (Figure 9A and C). Therefore, we concluded that one of the molecules affected by Ang1 for enlargement of the capillary was apelin in ECs.

### *Apelin induces an enlarged endothelial sheet in P-Sp culture system*

*In vivo* analysis suggested that apelin regulates the caliber change of blood vessels. Next, we observed blood vessel formation by using *in vitro* (P-Sp) organ culture system, which has previously been shown to mimic *in vivo* vasculogenesis and angiogenesis (Takakura *et al*, 1998, 2000). P-Sp explants from mice at E9.5 contain early developed DA. In the P-Sp culture system, ECs show two different morphologies. One is a sheet-like structure (vascular bed) that develops in the early stages of the culture. The other is a network-like structure, constructed from the ECs sprouting from the vascular bed. Previously, we identified that the sheet-like formation mimics vasculogenesis and the network formation mimics angiogenesis, which is a process of capillary sprouting from pre-existing vessels (Takakura *et al*, 2000). Therefore, as apelin-mutant embryos showed narrow ISVs, which were sprouted from the DA, this suggests that the P-Sp culture system can reproduce the *in vivo* effects of apelin.

In the P-Sp culture system, OP9 stromal cells were used as feeder cells for P-Sp explants. We induced apelin expression on OP9 cells (Figure 3B) and observed the effect. Compared to the control culture (Figure 10Aab), network-forming ECs became thick and the vascular density of the network area was high (Figure 10Acd), although the amount of branching was the same. By contrast, the suppression of apelin/APJ function, by blocking antibody against apelin, induced thin network formation by ECs (Figure 10Aef). When the network-forming area of ECs was evaluated, it was higher in apelin-expressing OP9 cells (OP9/apelin) than in control OP9 cells (OP9/vector); this effect by apelin was completely blocked by anti-apelin mAb (Figure 10Ag).

In the P-Sp culture system, we found that APJ is expressed in the network-forming ECs sprouted from the vascular bed as observed in the ISVs, but not in the ECs forming the sheet (Figure 10B). *In vitro* analysis indicated that the apelin/APJ system might affect cell-to-cell aggregation or assembly, and therefore we stained network-forming ECs by anti-VE-cadherin antibody. As observed in Figure 10C, apelin enhanced the assembly of ECs. Interestingly, in the control P-Sp culture, the network-forming endothelial layer, composed of one or two ECs, migrated in a peripheral direction along with the ECs at the tip (Figure 10Cab). On the other hand, when apelin was overexpressed on OP9 cells, many aggregated

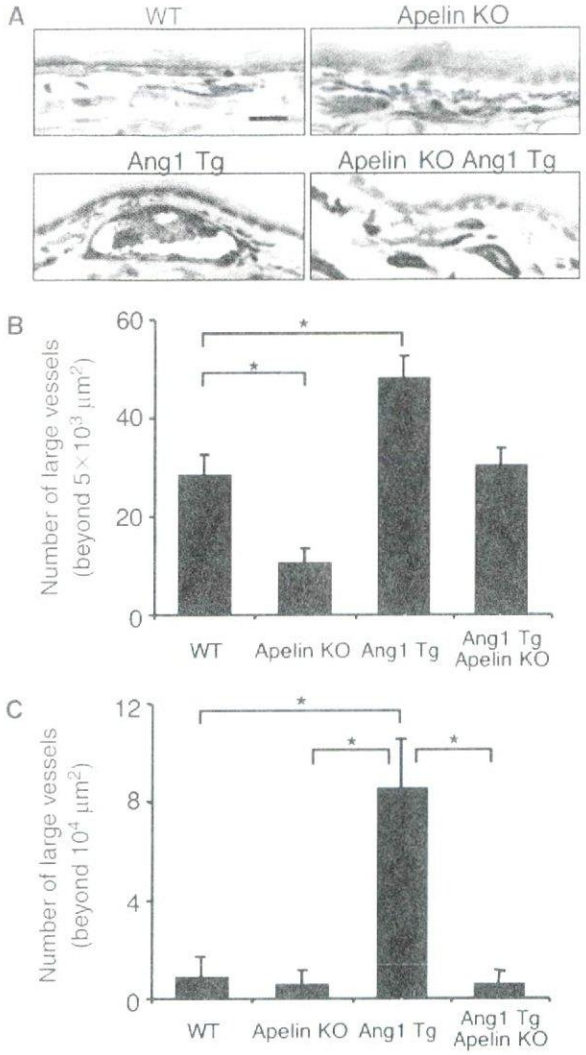


**Figure 9** Apelin/APJ system is involved in Ang1-induced vascular enlargement. (**A**) Sections of ear skin stained with anti-CD31 mAb. Ear skin was prepared from 8-week-old WT, apelin-deficient (apelin KO), Ang1Tg mice, or apelin-deficient mice mated with Ang1Tg mice (apelin KO/Ang1 Tg). Scale bar indicates 30 μm. (**B**, **C**) Quantitative evaluation of the number of enlarged blood vessels composed of a luminal cavity of more than 5000 μm$^2$ (B) or more than $10^4$ μm$^2$ (C) in the skin from mice as described in (A). Thirty random fields were observed from sections of three independent mice as described in (A). *$P<0.01$.

ECs migrated along with the ECs at the tip (Figure 10Ccd), and this effect was completely suppressed by anti-apelin mAb (Figure 10Cef). These results indicated that apelin induces an enlarged endothelial sheet when angiogenesis is taking place.

## Discussion

The knowledge of how vascular cells commit from their progenitor cells and generate a closed cardiovascular circulatory system has accumulated in recent years, mostly by the isolation and functional analysis of molecules associated with blood vessel formation. However, little is known regarding the molecular events that regulate EC morphogenesis, especially the caliber size determination of blood vessels. Data documented here, from both *in vitro* and *in vivo* analysis, showed that apelin regulates the enlargement of newly developed blood vessels during angiogenesis.

In angiogenesis, how blood vessels 'decide' their appropriate size is very important to the organization of the adjustment of tissue and organ demand for oxygen and nutrients. Our analysis clearly showed that APJ expression was induced by VEGF, which, in turn, is well known to be induced by tissue hypoxia (Liu *et al*, 1995). This indicates that, under tissue hypoxia, blood vessels have an opportunity to enlarge their size and the reduction of APJ expression finalizes the enlargement of blood vessel caliber under tissue normoxia. Indeed, in the retina, APJ was observed temporally in the radial vessels and the associated capillaries of retina from day 3 to day 12 after birth, but APJ expression on ECs was attenuated in the later stage (Saint-Geniez *et al*, 2002). As reported in the retina, we also found that APJ expression was observed in ECs sprouted from the DA and ECs on blood vessels in the neonatal dermis of mice (data not shown), but that it gradually disappeared with maturity. These expression patterns strongly suggested that APJ plays a spatio-temporal role in the maturation of blood vessels by transient expression on ECs of blood vessels where angiogenesis is taking place. Therefore, we concluded that one of the molecules associated with the regulation of blood vessel diameter was apelin in the ECs.

Based on our results presented here, it appears that VEGF, Ang1 and apelin regulate caliber size in a concerted fashion, as follows. Upon stimulation by VEGF, ECs sprouted from pre-existing vessels may express APJ. Subsequently, Ang1 stimulates these sprouted ECs to induce apelin expression. In the presence of both VEGF and apelin, the ECs start to proliferate, adhere and form contacts with each other through junctional proteins, and construct enlarged blood vessels. Apelin has been reported to induce angiogenesis in the Matrigel plug assay (Kasai *et al*, 2004) and also chemotaxis (Cox *et al*, 2006). In our experiments using the Matrigel plug assay, we found that apelin induced migration, rather than proliferation, of ECs (Supplementary Figure 14). Moreover, we confirmed that like VEGF, apelin modified the cytoskeleton structure (Supplementary Figure 15). Therefore, apelin may induce mobilization of ECs in the process of EC-to-EC assembly.

As we found, apelin deficiency suppressed the enlargement of ISVs during early embryogenesis. Furthermore, it has been reported elsewhere that Ang1 and VEGF are expressed in intersomitic or somitic tissues (Davis *et al*, 1996; Lawson *et al*, 2002) and that apelin is coexpressed with APJ-positive ECs in ISVs. Indeed both Tie2 and Ang1 mutant embryos showed impaired ISV formation (Dumont *et al*, 1994; Sato *et al*, 1995). Therefore, it appears that these three components may be involved in the regulation of caliber size change of the ISVs.

Transgenic overexpression of Ang1 in the keratinocyte induced enlarged blood vessels in the dermis (Suri *et al*, 1998) and administration of a potent Ang1 variant was also reported to induce enlargement of blood vessels (Cho *et al*, 2005; Thurston *et al*, 2005). Therefore, Ang1 expression may be a key determinant of caliber size during angiogenesis. Ang1 is usually produced from MCs in cells composing blood vessels (Davis *et al*, 1996), However, we previously reported that hematopoietic stem cells (HSCs) producing Ang1 migrate into avascular areas before the ECs start to migrate, and that this Ang1 from HSCs induces angiogenesis by promoting the chemotaxis of ECs (Takakura *et al*, 2000). Moreover, recently,

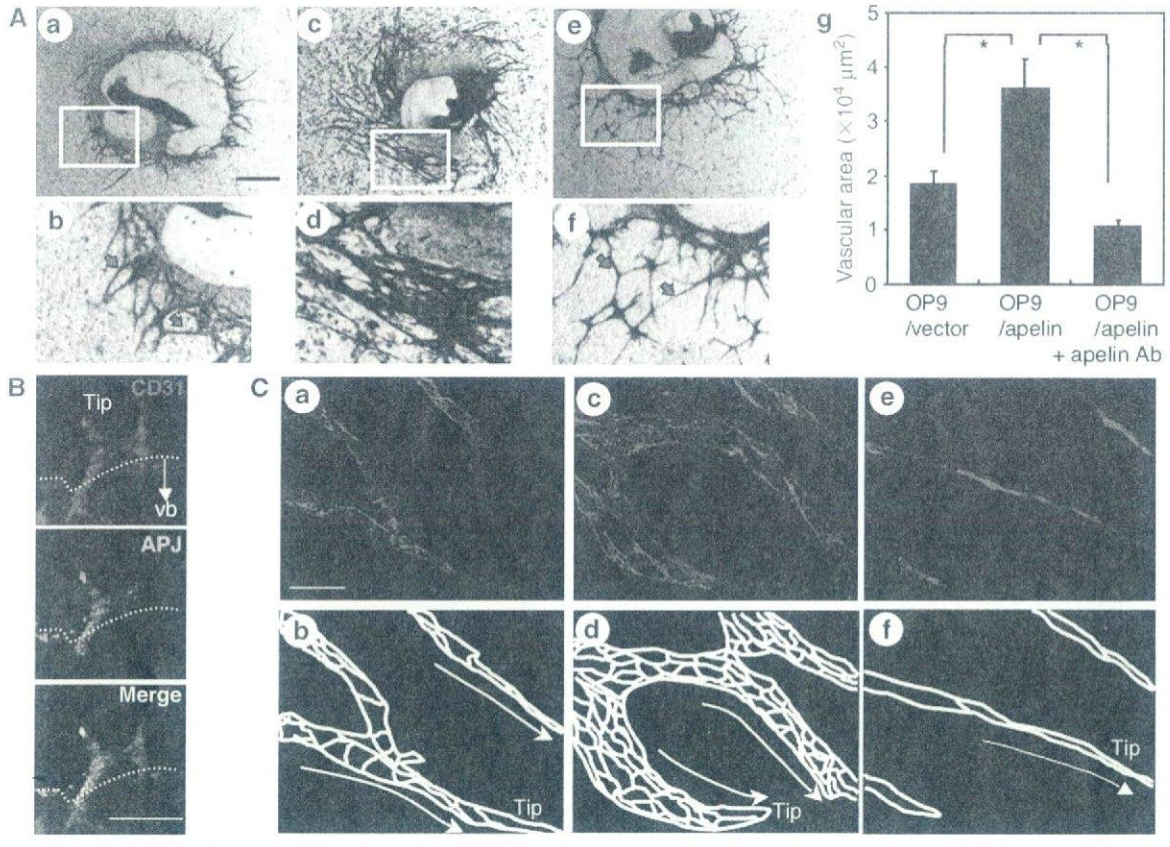


**Figure 10** Effect of apelin on the P-Sp culture system. (**A**) Effect of apelin on the network-like structure of ECs in the P-Sp culture system. P-Sp explants from E9.5 mouse embryos were cultured for 7 days on OP9/vector (a, b) or OP9/apelin, in the presence of B220 control mAbs (c, d) or anti-apelin mAbs (e, f), and then stained with anti-CD31 mAb. (b), (d) and (f) are higher magnifications of areas indicated by the box in (a), (c) and (e), respectively. Arrows indicate network-forming ECs. Scale bar indicates 1 mm (a, c, e) or 200 μm (b, d, f). (g) Quantitative evaluation of the vascular network area cultured as above. Endothelial space per 500 μm length of network-forming ECs was measured in 10 random fields. $^{*}P<0.001$. (**B**) Expression of APJ in ECs of P-Sp culture. Cells on culture plates were stained with anti-CD31 (red) and anti-APJ (green) antibodies. Tip, tip EC. Dotted line indicates the border of the vascular bed (vb). Note APJ expressed on ECs forming a network-like structure. Scale bar indicates 100 μm. (**C**) Network-forming ECs derived from P-Sp explants cultured on OP9/vector (a, b), OP9/apelin in the presence of control B220 mAbs (c, d) or OP9/apelin in the presence of anti-apelin mAbs (e, f) for 7 days were stained with anti-VE-cadherin (red) mAbs. Scale bar indicates 20 μm. Because nuclear staining cannot distinguish the nuclei of ECs from those of OP9 cells, only VE-cadherin expression was revealed. Therefore, the EC-to-EC boundary expressed by VE-cadherin is presented (b, d, f). Tip, tip EC. Migration direction of tip EC is indicated by the arrow.

we found that HSCs induce enlargement of blood vessels observed in the fibrous cap surrounding tumors (Okamoto *et al*, 2005) and Ang1 from HSCs in embryos, as well as adults, induces structural stability of newly developed blood vessels as a physiological function during angiogenesis (Yamada and Takakura, 2006). Therefore, it is possible that Ang1 from the HSC population, which are frequently observed in ischemic regions, is the one source of Tie2 activation and results in the production of apelin from ECs.

It has been suggested that apelin mediates phosphorylation and activation of endothelial NO synthase in ECs, causing NO release from ECs (Tatemoto *et al*, 2001; Ishida *et al*, 2004). NO is well known to induce relaxation of MCs, resulting in dilation of blood vessels. Therefore, it is possible that apelin causes endothelium-dependent vasodilatation by triggering the release of NO from ECs. In our analysis, however, we observed that apelin induced enlarged cord formation of HUVECs on Matrigel, and enlarged spheroids of HUVECs in the liquid culture. These culture conditions do not contain MCs, which indicates that apelin can induce enlargement of blood vessels without affecting MCs.

Knockout studies of the apelin gene suggested that molecular cues other than apelin rescue the narrow caliber size of blood vessels by compensational upregulation, because in the early stage of embryogenesis the narrow caliber of ISVs, observed in apelin-mutant embryos, was rescued in the later stage (data not shown). As observed in apelin knockout mice, APJ mutant mice appeared healthy as adults (Ishida *et al*, 2004); however, the requisite role of the apelin/APJ system in blood vessel formation was reported in *Xenopus* (Cox *et al*, 2006; Inui *et al*, 2006). The reason of this discrepancy is not known, but functionally redundant ligand/receptor or signalling pathways may be present in mice.

Tube formation is a fundamental mechanism for organ and tissue generation in most major organs, such as lung and kidney, as well as the vasculature. The molecular mechanism involved in tube generation is not clearly understood. During angiogenesis, neovessels must be generated by both single cell hollowing and cord hollowing methods. Through the analysis of the precise functional relationship between the molecules described above including the apelin/APJ system, anatomically described diverse tube formation of the vasculature will be further clarified at the molecular level.

## Materials and methods

### *Animals*

C57BL/6 mice and ICR mice were purchased from Japan SLC (Shizuoka, Japan) at 8 weeks of age and used between 8 and 12 weeks of age. Ang1Tg mice (Suri *et al*, 1998) with a C57BL/6 background were provided by Dr GD Yanchopoulos (Regeneron Pharmaceuticals Inc., Tarrytown, NY). Animal care in our laboratory was in accordance with the guidelines of Kanazawa and Osaka University for animal and recombinant DNA experiments.

### *Plasmids and transfection*

The mouse *Apelin* gene was cloned into the pCAGSIH expression vector. Lipofectamine Plus reagent (Invitrogen Life Technologies, Carlsbad, CA) was used to transfect cells with this plasmid and clones of cells exhibiting stable transfection were obtained by antibiotic resistance selection using G418 (Gibco, Grand Island, NY). Primer pairs for PCR to detect transfected gene are listed in Supplementary Table S1.

### *Tissue preparation, immunohistochemistry and flow cytometry*

Tissue fixation, preparation of tissue sections and staining of sections or cultured cells with antibodies were performed as described previously (Takakura *et al*, 2000). An biotin-conjugated anti-CD31 mAb (Pharmingen, San Diego, CA), anti-apelin Ab (4G5; Kawamata *et al*, 2001) and anti-APJ polyclonal Ab were used in the staining of tissue sections or cultured cells. To obtain a specific antibody against mouse APJ, a rabbit was immunized with a synthetic peptide (CHEKSIPYSQETLVD) derived from the C-terminal region of APJ. Antisera were affinity purified with the same peptide. Preimmunized rabbit immunoglobulins were used as a negative control to confirm specific staining. Sections were counterstained with hematoxylin or propidium iodide. The sections were observed using an Olympus IX-70 microscope (Olympus, Tokyo, Japan) and images were acquired with a CoolSnap digital camera (Roper Scientific, Trenton, NJ). Whole-mount immunohistochemistry using anti-CD31 mAb or anti-APJ was performed as previously described (Takakura *et al*, 1998). Stained embryos were observed under a Leica MZ16FA stereomicroscope (Leica, Solms, Germany) and photographed with a DC120 digital camera (Pixera, Los Gatos, CA). In all assays, we used an isotype-matched control Ig as a negative control and confirmed that the positive signals were not derived from nonspecific background. Investigation of the density and morphology of microvessels in lectin-stained whole mount of tracheal blood vessels was performed as described (Yamada and Takakura, 2006). In brief, after anaesthesia with sodium pentobarbital, mice were injected into the tail vein with fluorescein-labelled *Lycopersicon esculentum* lectin (Vector Laboratories, Burlingame, CA), which binds uniformly to the luminal surface of ECs and adherent leukocytes. Lectin-stained tracheas were removed from apelin-deficient and WT mice and analysed under a fluorescence microscope. Images were processed using Adobe Photoshop 6.0 software (Adobe Systems, San Jose, CA). Flow cytometric analysis was performed as previously described (Yamada and Takakura, 2006). FITC-conjugated anti-CD45 mAb and PE-conjugated anti-CD31 mAb (Pharmingen) were used. The stained cells were analysed by FACS Calibur (Becton Dickinson, Franklin Lakes, NJ) and sorted by EPICS flow cytometer (ALTRA; Beckman Coulter, Fullerton, CA).

### *Cell culture*

$4 \times 10^5$ HUVECs were cultured in six-well plates for 12 h in Humedia EG2 (Kurabo, Osaka, Japan). Cells were then incubated in M199 medium supplemented with 1% fetal bovine serum (FBS). After 3 h of serum deprivation, cells were incubated with basal medium containing 500 ng/ml of Ang1 (R&D Systems, Minneapolis, MN), 100 ng/ml of apelin (Bachem, Bubendorf, Switzerland) or 20 ng/ml of VEGF-$A_{165}$ (PeproTech, Rocky Hill, NJ).

The culture of P-Sp explant was performed as previously reported (Takakura *et al*, 2000). OP9 cells stably transfected with a pCAGSIH expression vector carrying the cDNA for mouse apelin or mock vector were used as feeder cells (OP9/apelin or OP9/vector, respectively) in the presence or absence of anti-apelin monoclonal blocking antibody (4G5; see Supplementary Figure 16 for functional analysis of this antibody in the inhibition of the apelin/APJ system) or control anti-B220 mAb. After 7 days of culture, the cultured cells on OP9 cells were fixed and stained with mAbs. For the culture of dissociated ECs from the AGM region, the regions were excised from E11.5 ICR embryos and dissociated by dispase II (Boehringer Mannheim, Mannheim, Germany) as previously described (Yamada and Takakura, 2006). Cells were suspended in DMEM supplemented with 15% fetal calf serum and cultured in OP9/vector or OP9/apelin seeded on 24-well plates in the presence of murine SCF (100 ng/ml; PeproTech), bFGF (1 ng/ml; R&D Systems) and OSM (10 ng/ml; R&D Systems). To this culture, we added 10 μg/ml anti-apelin or anti-B220 mAb. After 6 days of culture, the cells were fixed and double stained with anti-CD31 mAb and anti-VE-cadherin mAb (BD Pharmingen, San Jose, CA), or anti-CD31 mAb and claudin5 mAb (Abcam Inc., Cambridge, MA). Stained samples were analysed by confocal laser scanning microscopy (LSM510, Carl Zeiss, Germany). For the evaluation of apelin in promoting proliferation of HUVECs, HUVECs were cultured for 24 h in medium plus growth supplements and then for an additional 48 h in medium with or without apelin (10–100 ng/ml), VEGF (10 ng/ml) or apelin plus VEGF. Cell proliferation was then evaluated by directly counting the cell number.

### *Aortic ring culture for angiogenesis assay*

Descending thoracic aortas were isolated from apelin-deficient mice. Under a stereomicroscope, multiple 1-mm-thick aortic rings were prepared. Rings were then placed between two layers of type I collagen gel (Cellmatrix Type IA, Nitta Zeratin, Osaka, Japan), supplemented with Medium 199, 20% FBS in the presence or absence of VEGF (20 ng/ml) or apelin (200 ng/ml). The cultures were kept at 37 C in a humidified environment for a week and examined every second day under an Olympus microscope (IX70).

### *Statistical analysis*

All data are presented as mean ± standard deviation (s.d.). For statistical analysis, the statcel2 software package (OMS) was used with analysis of variance performed on all data followed by Tukey–Kramer multiple comparison test. When only two groups were compared, two-sided Student's *t*-test was used.

### *Supplementary data*

Supplementary data are available at *The EMBO Journal* Online (http://www.embojournal.org).

## Acknowledgements

We thank Dr GD Yanchopoulos (Regeneron Pharmaceuticals Inc.) and Dr Y Oike (Keio University, Tokyo, Japan) for providing us with Ang1Tg mice and with anti-LYVE-1 antibody, respectively. Moreover, we thank N Fujimoto for preparation of plasmid DNA and K Fukuhara for administrative assistance. This work was partly supported by a Grant-in-Aid from The Ministry of Education, Culture, Sports, Science and Technology of Japan to NT.

## References

Adams RH, Wilkinson GA, Weiss C, Diella F, Gale NW, Deutsch U, Risau W, Klein R (1999) Roles of ephrinB ligands and EphB receptors in cardiovascular development: demarcation of arterial/venous domains, vascular morphogenesis, and sprouting angiogenesis. *Genes Dev* **13:** 295–306

Ashley EA, Powers J, Chen M, Kundu R, Finsterbach T, Caffarelli A, Deng A, Eichhorn J, Mahajan R, Agrawal R, Greve J, Robbins R, Patterson AJ, Bernstein D, Quertermous T (2005) The endogenous peptide apelin potently improves cardiac contractility and reduces cardiac loading *in vivo*. *Cardiovasc Res* **65:** 73–82

Carmeliet P (2003) Angiogenesis in health and disease. *Nat Med* **9:** 653–660

Cho CH, Kim KE, Byun J, Jang HS, Kim DK, Baluk P, Baffert F, Lee GM, Mochizuki N, Kim J, Jeon BH, McDonald DM, Koh GY

(2005) Long-term and sustained COMP-Ang1 induces long-lasting vascular enlargement and enhanced blood flow. *Circ Res* **97:** 86–94

Cox CM, D'Agostino SL, Miller MK, Heimark RL, Krieg PA (2006) Apelin, the ligand for the endothelial G-protein-coupled receptor, APJ, is a potent angiogenic factor required for normal vascular development of the frog embryo. *Dev Biol* **296:** 177–189

Croitoru-Lamoury J, Guillemin GJ, Boussin FD, Mognetti B, Gigout LI, Cheret A, Vaslin B, Le Grand R, Brew BJ, Dormont D (2003) Expression of chemokines and their receptors in human and simian astrocytes: evidence for a central role of TNF alpha and IFN gamma in CXCR4 and CCR5 modulation. *Glia* **41:** 354–370

Davis S, Aldrich TH, Jones PF, Acheson A, Compton DL, Jain V, Ryan TE, Bruno J, Radziejewski C, Maisonpierre PC, Yancopoulos GD (1996) Isolation of angiopoietin-1, a ligand for the TIE2 receptor, by secretion-trap expression cloning. *Cell* **87:** 1161–1169

De Mota N, Reaux-Le Goazigo A, El Messari S, Chartrel N, Roesch D, Dujardin C, Kordon C, Vaudry H, Moos F, Llorens-Cortes C (2004) Apelin, a potent diuretic neuropeptide counteracting vasopressin actions through inhibition of vasopressin neuron activity and vasopressin release. *Proc Natl Acad Sci USA* **101:** 10464–10469

Devic E, Paquereau L, Vernier P, Knibiehler B, Audigier Y (1996) Expression of a new G protein-coupled receptor X-msr is associated with an endothelial lineage in *Xenopus laevis*. *Mech Dev* **59:** 129–140

Devic E, Rizzoti K, Bodin S, Knibiehler B, Audigier Y (1999) Amino acid sequence and embryonic expression of msr/apj, the mouse homolog of *Xenopus* X-msr and human APJ. *Mech Dev* **84:** 199–203

Dumont DJ, Gradwohl G, Fong GH, Puri MC, Gerstenstein M, Auerbach A, Breitman ML (1994) Dominant-negative and targeted null mutations in the endothelial receptor tyrosine kinase, tek, reveal a critical role in vasculogenesis of the embryo. *Genes Dev* **8:** 1897–1909

Edinger AL, Hoffman TL, Sharron M, Lee B, Yi Y, Choe W, Kolson DL, Mitrovic B, Zhou Y, Faulds D, Collman RG, Hesselgesser J, Horuk R, Doms RW (1998) An orphan seven-transmembrane domain receptor expressed widely in the brain functions as a coreceptor for human immunodeficiency virus type 1 and simian immunodeficiency virus. *J Virol* **72:** 7934–7940

Ferrara N, Alitalo K (1999) Clinical applications of angiogenic growth factors and their inhibitors. *Nat Med* **5:** 1359–1364

Ferrara N, Gerber HP, LeCouter J (2003) The biology of VEGF and its receptors. *Nat Med* **9:** 669–676

Gale NW, Yancopoulos GD (1999) Growth factors acting via endothelial cell-specific receptor tyrosine kinases: VEGFs, angiopoietins, and ephrins in vascular development. *Genes Dev* **13:** 1055–1066

Gerhardt H, Betsholtz C (2003) Endothelial-pericyte interactions in angiogenesis. *Cell Tissue Res* **314:** 15–23

Inui M, Fukui A, Ito Y, Asashima M (2006) Xapelin and Xmsr are required for cardiovascular development in *Xenopus laevis*. *Dev Biol* **298:** 188–200

Ishida J, Hashimoto T, Hashimoto Y, Nishiwaki S, Iguchi T, Harada S, Sugaya T, Matsuzaki H, Yamamoto R, Shiota N, Okunishi H, Kihara M, Umemura S, Sugiyama F, Yagami K, Kasuya Y, Mochizuki N, Fukamizu A (2004) Regulatory roles for APJ, a seven-transmembrane receptor related to angiotensin-type 1 receptor in blood pressure *in vivo*. *J Biol Chem* **279:** 26274–26279

Jain RK (2005) Normalization of tumor vasculature: an emerging concept in antiangiogenic therapy. *Science* **307:** 58–62

Kasai A, Shintani N, Oda M, Kakuda M, Hashimoto H, Matsuda T, Hinuma S, Baba A (2004) Apelin is a novel angiogenic factor in retinal endothelial cells. *Biochem Biophys Res Commun* **325:** 395–400

Katugampola SD, Maguire JJ, Matthewson SR, Davenport AP (2001) [(125)I]-(Pyr(1))Apelin-13 is a novel radioligand for localizing the APJ orphan receptor in human and rat tissues with evidence for a vasoconstrictor role in man. *Br J Pharmacol* **132:** 1255–1260

Kawamata Y, Habata Y, Fukusumi S, Hosoya M, Fujii R, Hinuma S, Nishizawa N, Kitada C, Onda H, Nishimura O, Fujino M (2001) Molecular properties of apelin: tissue distribution and receptor binding. *Biochim Biophys Acta* **1538:** 162–171

Kleinz MJ, Davenport AP (2004) Immunocytochemical localization of the endogenous vasoactive peptide apelin to human vascular and endocardial endothelial cells. *Regul Pept* **118:** 119–125

Koller A, Huang A (1999) Development of nitric oxide and prostaglandin mediation of shear stress-induced arteriolar dilation with aging and hypertension. *Hypertension* **34:** 1073–1079

Korff T, Augustin HG (1998) Integration of endothelial cells in multicellular spheroids prevents apoptosis and induces differentiation. *J Cell Biol* **143:** 1341–1352

Lawson ND, Vogel AM, Weinstein BM (2002) sonic hedgehog and vascular endothelial growth factor act upstream of the Notch pathway during arterial endothelial differentiation. *Dev Cell* **3:** 127–136

Lindahl P, Johansson BR, Leveen P, Betsholtz C (1997) Pericyte loss and microaneurysm formation in PDGF-B-deficient mice. *Science* **277:** 242–245

Liu Y, Cox SR, Morita T, Kourembanas S (1995) Hypoxia regulates vascular endothelial growth factor gene expression in endothelial cells. Identification of a 5′ enhancer. *Circ Res* **77:** 638–643

Masri B, Knibiehler B, Audigier Y (2005) Apelin signalling: a promising pathway from cloning to pharmacology. *Cell Signal* **17:** 415–426

O'Dowd BF, Heiber M, Chan A, Heng HH, Tsui LC, Kennedy JL, Shi X, Petronis A, George SR, Nguyen T (1993) A human gene that shows identity with the gene encoding the angiotensin receptor is located on chromosome 11. *Gene* **136:** 355–360

Oettgen P (2001) Transcriptional regulation of vascular development. *Circ Res* **89:** 380–388

Okamoto R, Ueno M, Yamada Y, Takahashi N, Sano H, Suda T, Takakura N (2005) Hematopoietic cells regulate the angiogenic switch during tumorigenesis. *Blood* **105:** 2757–2763

Risau W (1997) Mechanisms of angiogenesis. *Nature* **386:** 671–674

Saint-Geniez M, Masri B, Malecaze F, Knibiehler B, Audigier Y (2002) Expression of the murine msr/apj receptor and its ligand apelin is upregulated during formation of the retinal vessels. *Mech Dev* **110:** 183–186

Sato TN, Tozawa Y, Deutsch U, Wolburg-Buchholz K, Fujiwara Y, Gendron-Maguire M, Gridley T, Wolburg H, Risau W, Qin Y (1995) Distinct roles of the receptor tyrosine kinases Tie-1 and Tie-2 in blood vessel formation. *Nature* **376:** 70–74

Scott IC, Masri B, D'Amico LA, Jin SW, Jungblut B, Wehman AM, Baier H, Audigier Y, Stainier DY (2007) The G protein-coupled receptor agtrl1b regulates early development of myocardial progenitors. *Dev Cell* **12:** 403–413

Simon MC (2004) Vascular morphogenesis and the formation of vascular networks. *Dev Cell* **6:** 479–482

Suri C, Jones PF, Patan S, Bartunkova S, Maisonpierre PC, Davis S, Sato TN, Yancopoulos GD (1996) Requisite role of angiopoietin-1, a ligand for the Tie-2 receptor, during embryonic angiogenesis. *Cell* **87:** 1171–1180

Suri C, McClain J, Thurston G, McDonald DM, Zhou H, Oldmixon EH, Sato TN, Yancopoulos GD (1998) Increased vascularization in mice overexpressing angiopoietin-1. *Science* **282:** 468–471

Szokodi I, Tavi P, Foldes G, Voutilainen-Myllyla S, Ilves M, Tokola H, Pikkarainen S, Piuhola J, Rysa J, Toth M, Ruskoaho H (2002) Apelin, the novel endogenous ligand of the orphan receptor APJ, regulates cardiac contractility. *Circ Res* **91:** 434–440

Takakura N, Huang XL, Naruse T, Hamaguchi I, Dumont DJ, Yancopoulos GD, Suda T (1998) Critical role of the TIE2 endothelial cell receptor in the development of definitive hematopoiesis. *Immunity* **9:** 677–686

Takakura N, Watanabe T, Suenobu S, Yamada Y, Noda T, Ito Y, Satake M, Suda T (2000) A role for hematopoietic stem cells in promoting angiogenesis. *Cell* **102:** 199–209

Tatemoto K, Hosoya M, Habata Y, Fujii R, Kakegawa T, Zou MX, Kawamata Y, Fukusumi S, Hinuma S, Kitada C, Kurokawa T, Onda H, Fujino M (1998) Isolation and characterization of a novel endogenous peptide ligand for the human APJ receptor. *Biochem Biophys Res Commun* **251:** 471–476

Tatemoto K, Takayama K, Zou MX, Kumaki I, Zhang W, Kumano K, Fujimiya M (2001) The novel peptide apelin lowers blood pressure via a nitric oxide-dependent mechanism. *Regul Pept* **99:** 87–92

Thurston G, Wang Q, Baffert F, Rudge J, Papadopoulos N, Jean-Guillaume D, Wiegand S, Yancopoulos GD, McDonald DM (2005) Angiopoietin 1 causes vessel enlargement, without angiogenic

sprouting, during a critical developmental period. *Development* **132:** 3317–3326

Wang HU, Chen ZF, Anderson DJ (1998) Molecular distinction and angiogenic interaction between embryonic arteries and veins revealed by ephrin-B2 and its receptor Eph-B4. *Cell* **93:** 741–753

Yamada Y, Takakura N (2006) Physiological pathway of differentiation of hematopoietic stem cell population into mural cells. *J Exp Med* **203:** 1055–1065

Zhong TP, Childs S, Leu JP, Fishman MC (2001) Gridlock signalling pathway fashions the first embryonic artery. *Nature* **414:** 216–220

nature
cell biology

# Differential function of Tie2 at cell–cell contacts and cell–substratum contacts regulated by angiopoietin-1

Shigetomo Fukuhara[1,6], Keisuke Sako[1], Takashi Minami[2], Kazuomi Noda[1], Hak Zoo Kim[3], Tatsuhiko Kodama[2], Masabumi Shibuya[4], Nobuyuki Takakura[5], Gou Young Koh[3] and Naoki Mochizuki[1,6]

**Tie2 belongs to the receptor tyrosine kinase family and functions as a receptor for Angiopoietin-1 (Ang1). Gene-targeting analyses of either *Ang1* or *Tie2* in mice reveal a critical role of Ang1–Tie2 signalling in developmental vascular formation. It remains elusive how the Tie2 signalling pathway plays distinct roles in both vascular quiescence and angiogenesis. We demonstrate here that Ang1 bridges Tie2 at cell–cell contacts, resulting in *trans*-association of Tie2 in the presence of cell–cell contacts. In clear contrast, in isolated cells, extracellular matrix-bound Ang1 locates Tie2 at cell–substratum contacts. Furthermore, Tie2 activated at cell–cell or cell–substratum contacts leads to preferential activation of Akt and Erk, respectively. Microarray analyses and real-time PCR validation clearly show the differential gene expression profile in vascular endothelial cells upon Ang1 stimulation in the presence or absence of cell–cell contacts, implying downstream signalling is dependent upon the spatial localization of Tie2.**

Vascular development is coordinated by endothelial-specific receptor tyrosine kinases and their ligands: vascular endothelial growth factor (VEGF)–VEGF-receptor (VEGFR), ephrin–Eph receptor, and angiopoietin (Ang)–Tie receptor [1]. The Tie1 and Tie2 receptors constitute the Tie receptor family. Gene-targeting analyses have revealed the essentiality of these vascular endothelial receptor tyrosine kinases for vascular formation [1]. Even after the establishment of vascular network, neovessel formation is observed in ischemic diseases and tumours.

Tie2 maintains the vascular integrity of mature vessels by enhancing endothelial barrier function[2–6] and inhibiting apoptosis of endothelial cells[7–9]. Tie2 functions as a receptor for Ang family proteins (Ang1–4). Mice overexpressing Ang1 develop vessels resistant to inflammatory agent-induced leakage[10,11]. Thus, quiescence of blood vessels is thought to be mediated by Ang1–Tie2 signalling. Tie2 signalling is also suggested to promote cell migration and to be involved in VEGF-induced neovascularization and pathological angiogenesis, as opposed to the maintenance of cell quiescence[12–18]. Consistently, Tie2 is not only tyrosine phosphorylated in the endothelium of normal adult tissues, but is also highly expressed in the endothelium of neovessels of regenerating organs and tumours[19,20].

In the quiescent vessels, the endothelial cells tightly contact each other and do not proliferate[19]. On the other hand, during angiogenesis, the cells that lose cell–cell contacts are allowed to proliferate and migrate, thereby resulting in sprouting and branching from the pre-existing vessels to form neovasculature[19]. At present, it is unknown how Tie2 signalling is involved in both vascular quiescence and angiogenesis. Thus, we investigated Ang1–Tie2 signalling in the presence or absence of vascular endothelial cell–cell contacts.

## RESULTS

### Ang1 induces the translocation of Tie2 at cell–cell contacts

To first elucidate how Tie2 signalling controls vascular quiescence, we examined the localization of Tie2 in confluent human umbilical vein endothelial cells (HUVECs). Tie2 was broadly expressed on the plasma membrane in unstimulated cells. After stimulation with either cartilage oligomeric matrix protein (COMP)–Ang1, a potent Ang1 variant [14], or native Ang1, Tie2 was accumulated at the cell–cell contacts marked by vascular endothelial cadherin (VE-cadherin) (Fig. 1a and Supplementary Information, Fig. S1a). Similar relocation of Tie2 was observed in human arterial endothelial cells (Supplementary Information, Fig. S1b). The relocation of Tie2 was observed within 5 min after the stimulation, becoming more prominent during 15–45 min (Supplementary Information, Fig. S1c). Tie2 was then gradually endocytosed and disappeared from cell–cell contacts. Re-exposure to COMP–Ang1 6 h after the first stimulation re-induced accumulation of Tie2 at cell–cell contacts (Supplementary Information, Fig. S1d–f). These findings indicate that Ang1 induces relocation of Tie2 to cell–cell contacts, which is also supported by time-lapse imaging of cells expressing Tie2 carboxy-terminally

[1]Department of Structural Analysis, National Cardiovascular Center Research Institute, 5-7-1 Fujishirodai, Suita, Osaka 565-8565, Japan. [2]The Research Center for Advanced Science and Technology, University of Tokyo, Laboratory for System Biology and Medicine, 4-6-1, Komaba, Meguro, Tokyo, 153-8904, Japan. [3]Biomedical Research Center and Department of Biological Sciences, Korea Advanced Institute of Science and Technology, Guseong-dong, Daejeon, 305-701, Korea. [4]Division of Genetics, Institute of Medical Science, University of Tokyo, 4-6-1 Shirokane-dai, Minato-ku, Tokyo 108-8639, Japan. [5]Department of Signal Transduction, Research Institute of Microbial Diseases, Osaka University, 3-1 Yamada-oka, Suita, Osaka, 565-0871, Japan.
[6]Correspondence should be addressed to S.F. or N.M. (e-mails: fuku@ri.ncvc.go.jp; nmochizu@ri.ncvc.go.jp)

Received 3 December 2007; accepted 29 February 2008; published online 20 April 2008; DOI: 10.1038/ncb1714

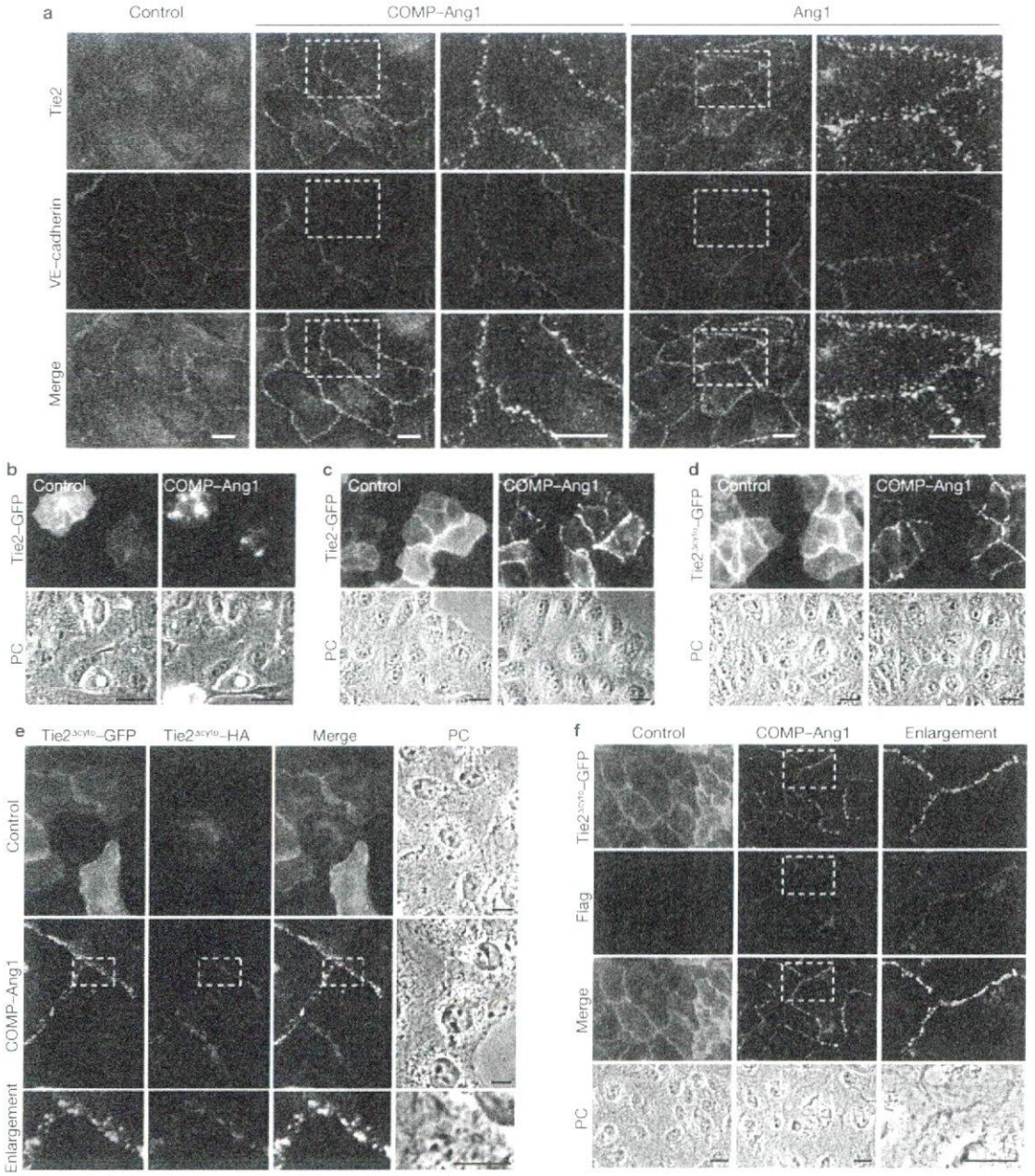


**Figure 1** Tie2 is recruited to cell–cell contacts upon Ang1 stimulation in vascular endothelial cells. (**a**) Confluent HUVECs plated on a collagen-coated dish (cells were plated on a collagen-coated dish for the following experiments unless otherwise indicated) were starved in medium 199 containing 0.5% BSA for 3 h and stimulated with vehicle (control), 200 ng ml$^{-1}$ COMP–Ang1, or 600 ng ml$^{-1}$ Ang1 for 20 min (COMP–Ang1 and native Ang1 were used at these concentrations throughout the following experiments unless otherwise indicated). After stimulation, the cells were fixed, immunostained with anti-Tie2 (top) and anti-VE-cadherin (middle) antibodies. Fluorescence images were obtained using an Olympus IX-81 inverted microscope. The boxed areas are enlarged on the right. (**b**) CHO cells transfected with the plasmid expressing Tie2–GFP were starved for 3 h and stimulated with COMP–Ang1. Tie2–GFP (top) and phase-contrast (PC, bottom) images of the Tie2–GFP-expressing cells surrounded by those that do not express Tie2–GFP were time-lapse imaged and analysed by MetaMorph 6.1 software. The images before (left) and 1 h after (right) stimulation are shown. (**c**) Tie2–GFP-expressing cells contacting each other were stimulated with COMP–Ang1 and time-lapse imaged. (**d**) CHO cells transfected with the plasmid expressing Tie2Δcyto–GFP were stimulated with COMP–Ang1 and time-lapse imaged. (**e**) CHO cells were transfected with either the plasmid expressing Tie2Δcyto–GFP or that expressing Tie2Δcyto–HA. The next day, the cells expressing Tie2Δcyto–GFP and those expressing Tie2Δcyto–HA were co-plated and stimulated with either vehicle (control) or COMP–Ang1 for 1 h. After stimulation, the cells were stained with anti-HA antibody. GFP (green), HA (red), the merged images, and the phase-contrast images (PC) are shown. The boxed areas are enlarged at the bottom of each image. (**f**) CHO cells transfected with the vector encoding Tie2Δcyto–GFP were stimulated as described in **e**. To visualize Flag-tagged COMP–Ang1, the stimulated cells were stained with anti-Flag antibody. GFP (green), Flag (red), the merged images (merge), and the phase-contrast images (PC) are shown as labelled on the left. The boxed areas are enlarged in the right panels. The scale bars represent 20 μm (**a**, **b**, **c**, **d**, **f**), and 10 μm (**e**), respectively.